Colloquium: Gravitational form factors of the proton

V. D. Burkert*
Thomas Jefferson National Accelerator Facility, Newport News, Virginia, USA

L. Elouadrhiri
Thomas Jefferson National Accelerator Facility, Newport News, Virginia, USA and Center of Nuclear Femtography, Newport News, Virginia, USA

F. X. Girod
Thomas Jefferson National Accelerator Facility, Newport News, Virginia, USA

C. Lorcé
CPHT, CNRS, École polytechnique, Institut Polytechnique de Paris, 91120 Palaiseau, France

P. Schweitzer
Department of Physics, University of Connecticut, Storrs, Connecticut 06269, USA

P. E. Shanahan
Center for Theoretical Physics, Massachusetts Institute of Technology, Cambridge, Massachusetts 02139, USA

(published 22 December 2023)

The physics of the gravitational form factors of the proton, as well as their understanding within quantum chromodynamics, has advanced significantly in the past two decades through both theory and experiment. This Colloquium provides an overview of this progress, highlights the physical insights unveiled by studies of gravitational form factors, and reviews their interpretation in terms of the mechanical properties of the proton.

DOI: 10.1103/RevModPhys.95.041002

CONTENTS

I. INTRODUCTION

This Colloquium reviews the recent theoretical and experimental progress in studies of the gravitational form factors of the proton and other hadrons, which has shed new light on the proton's structure and its mechanical properties. To place this

*Corresponding author: burkert@jlab.org

emerging area in context, the history of proton structure and its description in quantum chromodynamics are first reviewed.

A. Anomalous magnetic moment

Soon after the proton (Rutherford, 1919) and neutron (Chadwick, 1932) were established as the constituents of atomic nuclei, experiments showed that these spin-1/2 particles with nearly equal masses $M_N \simeq 940\ \mathrm{MeV}/c^2$ are not pointlike elementary fermions. If they were, the Dirac equation would predict the magnetic moment of the proton to be one nuclear magneton $\mu_N \equiv e\hbar/2M_N$, and that of an electrically neutral particle like the neutron to be zero. Instead, the proton magnetic moment was measured to be about $\mu_p \simeq 2.5\mu_N$ (Frisch and Stern, 1933). Later, the neutron magnetic moment was found to be $\mu_n \simeq -1.5\mu_N$ (Alvarez and Bloch, 1940); for the modern values of the magnetic moments, see Workman *et al.* (2022). These experiments have shown that the nucleon is not a pointlike elementary particle, giving birth in 1933 to the field of proton structure.

Protons and neutrons are hadrons, particles that feel the strong force, which is the strongest interaction known in nature. Based on approximate isospin symmetry, they are understood as partnered (isospin up and down) states, referred to collectively as the nucleon (Heisenberg, 1932). As the constituents of nuclei, nucleons are responsible for more than 99.9% of the mass of matter in the visible Universe and have naturally become the most experimentally studied objects in hadronic physics.

B. The proton's finite size

An important milestone in the field of nucleon structure was brought by studies of elastic electron-proton scattering, shown in Fig. 1(a), which revealed early insights into the proton's size. The deviations in scattering data from expectations for pointlike particles are encoded in terms of form factors (FFs) defined through matrix elements of the electromagnetic current operator $\langle p', \vec{s}'|J^{\mu}_{\mathrm{em}}|p, \vec{s}\rangle$, where $|p, \vec{s}\rangle$ is the initial state of the proton with momentum p polarized along the $\vec{s}$ direction. The final proton state is defined analogously.

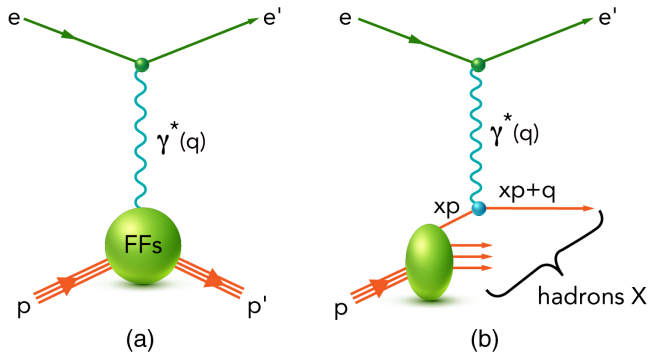

FIG. 1. (a) Elastic electron-proton scattering process in which the electromagnetic form factors (FFs) are measured. (b) Inclusive deep inelastic scattering (DIS) where the proton is dissociated into a final state consisting of unresolved hadrons. In the Bjorken limit $p \cdot q \to \infty$ and $Q^2 = -q^2 \to \infty$ with $x_B = Q^2/2p \cdot q$ fixed, DIS is interpreted in the so-called infinite-momentum frame as the scattering of electrons off pointlike quarks carrying the fraction x of the nucleon's momentum, where $x = x_B$ up to corrections suppressed by M_N^2/Q^2.

These FFs would be constants for pointlike particles, but they were found to be pronounced functions of the Mandelstam variable $t = (p' - p)^2$. A spin-1/2 particle has two electromagnetic FFs $F_1(t)$ and $F_2(t)$, defined such that $F_1(0)$ is the electric charge in units of e and $F_2(0)$ is the anomalous magnetic moment, i.e., the deviation from the value predicted by the Dirac equation, in units of μ_N. Knowledge of the t dependence of electromagnetic FFs allowed information about the spatial distributions of electric charge and magnetization to be inferred (Sachs, 1962); more discussion of this interpretation was given by Lorcé (2020) and Chen and Lorcé (2022, 2023). This led to the first determination of the proton charge radius of 0.74 ± 0.24 fm (McAllister and Hofstadter, 1956). These experiments have continued to this day, and using a variety of experimental techniques they resulted in a much more precise knowledge of the proton's charge radius (Workman *et al.*, 2022).

C. Discovery of partons

The 1950s witnessed monumental progress in accelerator and detection techniques followed by a proliferation of discoveries of strongly interacting particles and resonances, including particles like the antiproton, Δ, and Ξ; see the early review by Snow and Shapiro (1961). On the theoretical side, this led to the development of the quark model (Gell-Mann, 1964; Zweig, 1964), in which hadrons are classified according to quantum numbers that are understood to arise from various combinations of "quarks." The quarks in this model were group-theoretical objects, and their dynamics were unknown.

The next milestone was brought by high-energy experiments carried out at the Stanford Linear Accelerator, where the Bjorken scaling predicted on the basis of current algebra and dispersion relation techniques (Bjorken, 1969) was observed in inclusive deep inelastic scattering (DIS) (Bloom *et al.*, 1969). The response of the nucleon in DIS is described by structure functions that, on general grounds, are functions of the Lorentz invariants $p \cdot q$ and $Q^2 = -q^2$, where p^{μ} is the nucleon four-momentum and q^{μ} is the four-momentum transfer; see Fig. 1(b). Bjorken scaling is the property that, in the high-energy limit $p \cdot q \to \infty$ and $Q^2 \to \infty$ with their ratio fixed, the structure functions are, to a first approximation, functions of a single variable $x_B = Q^2/2p \cdot q$ that on kinematical grounds satisfies $0 < x_B < 1$.

The physical significance of this nontrivial observation was interpreted in the parton model (Feynman, 1969), where the DIS process proceeds as shown in Fig. 1(b), namely, the electrons scatter off nearly free electrically charged pointlike particles called partons, with a cross section that can be calculated in quantum electrodynamics (QED). The structure of the nucleon in DIS is described in terms of parton distribution functions (PDFs), depicted by the green ellipse in Fig. 1(b). (More precisely, PDFs are defined after squaring the amplitude in Fig. 1 and summing over the complete set of states X.) In modern terminology, the PDFs in unpolarized DIS are denoted as $f_1^a(x)$, with a labeling the type of parton. More precisely $f_1^a(x)\mathrm{d}x$ is the probability of finding a parton of type a in the initial state inside of a nucleon moving at

nearly the speed of light (an appropriate picture in DIS where $x \approx x_B$) and carrying a fraction of the nucleon's momentum in the interval $[x, x + \mathrm{d}x]$. It was soon realized that the electrically charged partons, identified as quarks and antiquarks, carry only half of the nucleon's momentum between them.

D. Colored quarks and gluons, QCD, and confinement

The discovery of proton substructure and the development of the parton model were key to establishing quantum chromodynamics (QCD) as the theory of the fundamental interaction between quarks carrying $N_c = 3$ different color charges (and antiquarks carrying the corresponding anticharges) (Fritzsch, Gell-Mann, and Leutwyler, 1973; Gross and Wilczek, 1973; Politzer, 1973). The color forces are mediated by the exchange of spin-1 gluons that also carry color charges (as opposed to electrically neutral photons that mediate interactions in QED). Evidence for the existence of gluons has been found in the study of e^+e^- annihilation processes (Brandelik *et al.*, 1980). Being electrically neutral, the gluons are "invisible" in interactions with electrons and account for the missing half of the proton momentum in DIS.

The QCD Lagrangian is given by

$$\mathcal{L} = \sum_q \bar{\psi}_q (i\not{D} + m_q)\psi_q - \tfrac{1}{4}F^2, \tag{1}$$

where $\bar{\psi}_q$ and ψ_q denote the quark and antiquark fields and m_q denotes the current quark masses. The summation runs over the quark flavors $q \in \{u, d, s, c, b, t\}$. The covariant derivative is defined as $iD_\mu = i\partial_\mu + gA^c_\mu T^c$ and $F^2 = F^c_{\mu\nu}F^{c\mu\nu}$, with $F^c_{\mu\nu} = \partial_\mu A^c_\nu - \partial_\nu A^c_\mu + gf^{cde}A^d_\mu A^e_\nu$. Here A^c_μ are the gauge (gluon) fields and T^c are the generators in the fundamental representation of $\mathrm{SU}(N_c)$, where $c \in \{1, \ldots, N_c^2 - 1\}$ and f^{cde} are the structure constants of the $\mathrm{SU}(N_c)$ group. Non-Abelian gauge theories like QCD are renormalizable ('t Hooft and Veltman, 1972) with the coupling constant $\alpha_s(\mu) = g(\mu)^2/4\pi$, depending on the renormalization scale μ. When it comes to describing hadrons, the scale is $\mu \sim 1$ GeV and $\alpha_s(\mu)$ is of the order of unity. The interaction is thus strong and the solution of Eq. (1) requires nonperturbative techniques. However, in high-energy processes such as DIS, where the renormalization scale is identified with the hard scale of the process, $\alpha_s(Q)$ decreases with increasing Q reaching $\alpha_s(91\ \mathrm{GeV}) \approx 0.12$ at the scale of the Z-boson mass. This property, known as asymptotic freedom, explains why quarks, antiquarks, and gluons appear in such reactions as nearly free partons to a first approximation. The fact that free color charges are never observed in nature gave rise to the confinement hypothesis, whose theoretical explanation is still an open question.

E. Proton mass, spin, and *D*-term

While the fundamental degrees of freedom and their interaction described in terms of the Lagrangian (1) are well established, many questions remain open. For instance, the proton and neutron quantum numbers arise from combining three light quarks uud and udd, whose masses in the QCD Lagrangian (1) are explained by the Brout-Englert-Higgs mechanism (Englert, 2014; Higgs, 2014). The smallness of $m_u \sim 2\ \mathrm{MeV}/c^2$ and $m_d \sim 5\ \mathrm{MeV}/c^2$, however, gives rise to one of the central questions of QCD, namely, how does the nucleon mass of 940 MeV/c^2 come about? [A widespread misconception is that $m_u + m_u + m_d \sim 9\ \mathrm{MeV}/c^2$ explains only about 1% of the proton mass. This is incorrect, as in QCD the quark mass contribution is due to the operator $m_q\bar{\psi}_q\psi_q$, which includes virtual quark-antiquark pair contributions, leading to a much larger fraction (about 10%–15%) of the proton mass, as discussed in Sec. II.D.]

Another central question concerns the proton spin. In a "static" quark model one would naively attribute the spin 1/2 of the nucleon to the spins of the quarks. In nature, owing to the relatively light u and d quarks being confined within distances of $\mathcal{O}(1\ \mathrm{fm})$, Heisenberg's uncertainty principle implies an ultrarelativistic motion of the quarks. The orbital motion of quarks is expected to play an important role in the spin budget of the nucleon. At the quantitative level, the nucleon spin decomposition is, however, still not precisely known (Ji, Yuan, and Zhao, 2021).

The answers to these questions lie in the matrix elements of the energy-momentum tensor (EMT), an operator in quantum field theory of central importance that is associated with the invariance of the theory under spacetime translations. These matrix elements encode key information, including the mass and spin of a particle, the less well-known but equally fundamental D-term (D stands for the German word *Druck*, meaning pressure), as well as information about the distributions of energy, angular momentum, and various mechanical properties such as internal forces inside the system. These properties are encoded in the gravitational form factors. In the standard model (plus gravity) the EMT couples to gravitons, so the direct way to measure its matrix elements would be graviton-proton scattering. Since the gravitational interaction between a proton and an electron is (at currently achievable lab energies) 10^{-39} times weaker than their electromagnetic interaction, the direct use of gravity to probe proton structure is impossible in electron-proton scattering, and in fact in any accelerator experiment in the foreseeable future. However, we have learned how to apply indirect methods to acquire information about the EMT through studies of hard exclusive reactions. The purpose of this Colloquium is to review the progress in theory, experiment, and interpretation of the EMT matrix elements. While the main focus here is on the proton, other hadrons are also discussed to provide a wider context and improve understanding.

II. ENERGY-MOMENTUM TENSOR

In this section, after reviewing the definition and properties of the EMT in QCD, the gravitational form factors (GFFs) of the proton are introduced. It is shown how GFFs can be leveraged to elucidate the proton's mass and spin decompositions.

A. Definition of the EMT operator

In QCD, the EMT $T^{\mu\nu} = \sum_q T^{\mu\nu}_q + T^{\mu\nu}_G$ can be decomposed into gauge-invariant quark and gluon parts as

$$\begin{aligned} T^{\mu\nu}_q &= \bar{\psi}_q \gamma^\mu i D^\nu \psi_q, \\ T^{\mu\nu}_G &= -F^{c\mu\lambda}F^{c\nu}_\lambda + \tfrac{1}{4}g^{\mu\nu}F^2, \end{aligned} \tag{2}$$

with $g_{\mu\nu} = \mathrm{diag}(+1,-1,-1,-1)$ the Minkowski metric. In quantum field theory, the expressions for the matrix elements of bare operators contain divergences and must be renormalized ('t Hooft and Veltman, 1972). Therefore, each term in Eq. (2) is understood as a renormalized operator defined at some renormalization scale μ. The components of the EMT are interpreted in the same way as in classical theory, namely, T^{00} is the energy density, T^{0i} is the momentum density, T^{i0} is the energy flux, and T^{ij} is the momentum flux or stress tensor.

Since the antisymmetric part $T^{[\mu\nu]} = (1/2)(T^{\mu\nu} - T^{\nu\mu})$ of Eq. (2) can be written as a total divergence using the equations of motion, it does not contribute to the total four-momentum and angular momentum of the system. In the literature, one often considers only the symmetric part $T^{\{\mu\nu\}} = (1/2)(T^{\mu\nu} + T^{\nu\mu})$, known as the Belinfante EMT (Belinfante, 1962), where the distinction between orbital angular momentum and spin is lost (Leader and Lorcé, 2014; Lorcé, Mantovani, and Pasquini, 2018).

B. Trace anomaly

The invariance of the classical Lagrangian of a theory under a certain symmetry implies the existence of a conserved, so-called Noether current (Noether, 1918). For instance, the EMT is the Noether current associated with the invariance of a theory under spacetime translations. If the classical symmetry is obeyed in quantum field theory (as is the case for spacetime translations), one obtains a conservation law.

If a classical symmetry is spoiled by quantum effects, then one speaks of a "quantum anomaly" and there is no associated conservation law. One important example is the trace anomaly (for another example see Sec. IV.A): the QCD Lagrangian (1) is approximately invariant under scale transformations $x \mapsto x' = \lambda x$ with arbitrary $\lambda > 0$. It is not an exact symmetry, since the divergence of the corresponding Noether current does not vanish but is equal at the classical level to $g_{\mu\nu}T^{\mu\nu}_{\mathrm{class}} = \sum_q m_q \bar{\psi}_q \psi_q$. In the light quark sector, owing to the smallness of the up- and down-quark masses, one would nevertheless expect this to be a good approximate symmetry that is similar to the isospin symmetry encountered in Sec. I.A. However, quantum corrections alter the trace of the EMT as (Collins, Duncan, and Joglekar, 1977; Nielsen, 1977)

$$g_{\mu\nu}T^{\mu\nu} = \sum_q (1+\gamma_m) m_q \bar{\psi}_q \psi_q + \frac{\beta(g)}{2g} F^2, \tag{3}$$

where γ_m is the anomalous quark mass dimension and $\beta(g) = \partial g/\partial \ln \mu$ is the QCD beta function that describes how the coupling changes with the renormalization scale. As later discussed, the trace anomaly plays an important role for the mass and mechanical properties of the proton. For more details, see Braun, Korchemsky, and Müller (2003), Hatta, Rajan, and Tanaka (2018), Tanaka (2019), and Ahmed, Chen, and Czakon (2023).

C. Definition of the proton gravitational form factors

The electromagnetic structure of the proton is encoded in the matrix elements of the electromagnetic current $\langle p', \vec{s}' | J^{\mu}_{\mathrm{em}} | p, \vec{s} \rangle$. Similarly, the matrix elements of the EMT operator $\langle p', \vec{s}' | T^{\mu\nu}_a | p, \vec{s} \rangle$ for quarks ($a = q$) and gluons ($a = G$) allow one to study the mass and spin decompositions, as well as the mechanical properties.

Thanks to Poincaré symmetry, these matrix elements can be written as (Kobzarev and Okun, 1962; Pagels, 1966; Ji, 1997b; Bakker, Leader, and Trueman, 2004; Lorcé, Schweitzer, and Tezgin, 2022)

$$\begin{aligned}
&\langle p', \vec{s}' | T^{\mu\nu}_a | p, \vec{s} \rangle \\
&= \bar{u}(p', \vec{s}') \left[A_a(t) \frac{P^\mu P^\nu}{M_N} \right. \\
&\quad + D_a(t) \frac{\Delta^\mu \Delta^\nu - g^{\mu\nu}\Delta^2}{4M_N} + \bar{C}_a(t) M_N g^{\mu\nu} \\
&\quad \left. + J_a(t) \frac{P^{\{\mu} i\sigma^{\nu\}\lambda} \Delta_\lambda}{M_N} - S_a(t) \frac{P^{[\mu} i\sigma^{\nu]\lambda} \Delta_\lambda}{M_N} \right] u(p, \vec{s}),
\end{aligned} \tag{4}$$

with $P = (p' + p)/2$ and $\Delta = p' - p$ the symmetric kinematical variables, $u(p, \vec{s})$ the usual free Dirac spinor, and M_N the nucleon mass. The Lorentz-invariant functions $A_a(t)$, $D_a(t)$, $\bar{C}_a(t)$, $J_a(t)$, and $S_a(t)$ depend on the square of the four-momentum transfer $t = \Delta^2$. They are the EMT analogs of the more familiar electromagnetic FFs and are accordingly called GFFs. In contrast to the electromagnetic FFs, these GFFs also inherit a renormalization-scale dependence from the associated operators, which is omitted in the notation for convenience. The total GFFs $\sum_a A_a(t)$, $\sum_a D_a(t)$, $\sum_a \bar{C}_a(t)$, and $\sum_a J_a(t)$ are, however, renormalization scale independent (Nielsen, 1977).

On top of restricting the number of GFFs, Poincaré symmetry imposes additional constraints, namely,

$$A(0) = \sum_q A_q(0) + A_G(0) = 1, \tag{5}$$

$$J(0) = \sum_q J_q(0) + J_G(0) = \tfrac{1}{2}, \tag{6}$$

$$\tfrac{1}{2}\Delta\Sigma = \sum_q S_q(0), \tag{7}$$

$$\bar{C}(t) = \sum_q \bar{C}_q(t) + \bar{C}_G(t) = 0, \tag{8}$$

where Eq. (5) follows from translation symmetry (Ji, 1998), while Eqs. (6) and (7) result from Lorentz symmetry (Ji, 1997b; Bakker, Leader, and Trueman, 2004), with $(1/2)\Delta\Sigma$ denoting the quark spin contribution to the nucleon spin. The constraint (8), which is valid for any t, follows from the EMT conservation $\partial_\mu T^{\mu\nu} = 0$. Note that the renormalization-scale-invariant quantity (Polyakov and Weiss, 1999)

$$D \equiv D(0) = \sum_q D_q(0) + D_G(0), \tag{9}$$

known as the D-term, is a global property of the proton (and in fact any hadron) whose value is not fixed by spacetime

symmetries (Polyakov and Weiss, 1999). Its physical interpretation is discussed in Sec. VI.

Until recently the only information about GFFs known from phenomenology was $A_a(0) = \int_{-1}^{1} \mathrm{d}x\, x f_1^a(x)$, which corresponds to the fraction of proton momentum carried by the partons a inferred from DIS experiments, and $S_q(0) = (1/2)\int_{-1}^{1} \mathrm{d}x\, g_1^q(x)$, where $g_1^q(x)$ is the quark helicity distribution (Aidala *et al.*, 2013).

D. Decomposition of proton mass

Just as the charge density is defined via a Fourier transform of the matrix elements of the electromagnetic current, the spatial distributions of energy and momentum read (Polyakov, 2003; Polyakov and Schweitzer, 2018b; Lorcé, Moutarde, and Trawiński, 2019)

$$\mathcal{T}_a^{\mu\nu}(\vec{r}) = \int \frac{\mathrm{d}^3\Delta}{(2\pi)^3 2E} e^{-i\vec{\Delta}\cdot\vec{r}} \langle p'|T_a^{\mu\nu}|p\rangle \tag{10}$$

in the so-called Breit frame defined by the conditions $\vec{p}' = -\vec{p} = \vec{\Delta}/2$ and $p'^0 = p^0 = E = \sqrt{M_N^2 + \vec{\Delta}^2/4}$. For ease of notation, the dependence on the nucleon polarization is omitted. Integrating over space, one obtains

$$\int \mathrm{d}^3 r \mathcal{T}_a^{\mu\nu}(\vec{r}) = \left.\frac{\langle p|T_a^{\mu\nu}|p\rangle}{2M_N}\right|_{\vec{p}=\vec{0}}, \tag{11}$$

i.e., the matrix elements for the proton at rest. More explicitly one finds that

$$\int \mathrm{d}^3 r \mathcal{T}_a^{\mu\nu}(\vec{r}) = \begin{pmatrix} U_a & 0 & 0 & 0 \\ 0 & W_a & 0 & 0 \\ 0 & 0 & W_a & 0 \\ 0 & 0 & 0 & W_a \end{pmatrix}. \tag{12}$$

The components $\mathcal{T}^{00}(\vec{r})$ and $(1/3)\sum_i \mathcal{T}^{ii}(\vec{r})$ represent the energy density and the isotropic pressure in the system. Thus, $U_a = \int \mathrm{d}^3 r\, \mathcal{T}_a^{00}(\vec{r}) = [A_a(0) + \bar{C}_a(0)]M_N$ and $W_a = (1/3)\sum_i \int \mathrm{d}^3 r\, \mathcal{T}_a^{ii}(\vec{r}) = -\bar{C}_a(0) M_N$ are, respectively, interpreted as the quark and gluon contributions to internal energy and pressure-volume work.

Since by definition $p^2 = M_N^2$, the proton mass can be identified with the total energy in the rest frame

$$\sum_a U_a = M_N. \tag{13}$$

Moreover, since the proton is a bound state at mechanical equilibrium, the virial theorem says that the total pressure-volume work must vanish (Laue, 1911; Lorcé, 2018a; Lorcé *et al.*, 2021)

$$\sum_a W_a = 0. \tag{14}$$

These are two independent sum rules underlying the various mass decompositions proposed in the literature; see Lorcé *et al.* (2021) for a detailed review. To keep the following discussion as simple as possible, the standard modified minimal subtraction ($\overline{\mathrm{MS}}$) scheme is used in the following, with the additional requirement that the trace anomaly arises purely from the gluonic sector (Metz, Pasquini, and Rodini, 2020; Lorcé *et al.*, 2021).

Defining the quark mass contribution to the nucleon mass via

$$M_m = \sum_q \sigma_q \equiv \left.\frac{\langle p|\sum_q m_q \bar{\psi}_q \psi_q|p\rangle}{2M_N}\right|_{\vec{p}=\vec{0}}, \tag{15}$$

one obtains a three-term mass decomposition directly from the energy sum rule (13),

$$M_N = \sum_q M_q + M_m + M_G, \tag{16}$$

where $M_q = U_q - \sigma_q$ and $M_G = U_G$ can be interpreted as the kinetic and potential energies of quarks and gluons, respectively (Metz, Pasquini, and Rodini, 2020; Rodini, Metz, and Pasquini, 2020). Motivated by the fact that the traceless part of the gluon EMT can be directly accessed in high-energy experiments, a further decomposition of the gluon energy

$$M_G = \bar{M}_G + \tfrac{1}{4} M_A \tag{17}$$

into the traceless part $\bar{M}_G = (3/4)(U_G + W_G) = (3/4)A_G(0)M_N$ and pure trace part $(1/4)M_A = (1/4)(U_G - 3W_G)$ was proposed by Ji (1995a, 1995b, 2021). Since at the classical level the gluon EMT is traceless, $\bar{M}_G$ was interpreted as the "classical" gluon energy and $(1/4)M_A$, with

$$M_A = \left.\frac{\langle p|\sum_q \gamma_m m_q \bar{\psi}_q \psi_q + [\beta(g)/2g]F^2|p\rangle}{2M_N}\right|_{\vec{p}=\vec{0}} \tag{18}$$

representing the "quantum anomalous energy." This interpretation, however, is not supported by a careful analysis in the $\overline{\mathrm{MS}}$ scheme. Indeed, at the level of renormalized operators it is the total gluon energy density (and not its traceless part) that has the familiar form $T_G^{00} = (1/2)(\vec{E}^2 + \vec{B}^2)$, ensuring that time translation symmetry remains exact under renormalization (Nielsen, 1977; Suzuki, 2013; Tanaka, 2019, 2023; Metz, Pasquini, and Rodini, 2020; Lorcé *et al.*, 2021; Ahmed, Chen, and Czakon, 2023). A recent explicit one-loop calculation within the scalar diquark model (Amor-Quiroz *et al.*, 2023) confirms that, unlike the EMT trace, the total energy does not receive any intrinsic anomalous contributions.

Since mass is a Lorentz-invariant quantity, one sometimes prefers to start with the trace of the EMT,

$$\langle p|g_{\mu\nu}T^{\mu\nu}|p\rangle = 2p^2 = 2M_N^2, \tag{19}$$

and then decompose it into quark and gluon contributions (Shifman, Vainshtein, and Zakharov, 1978; Donoghue, Golowich, and Holstein, 2014; Hatta, Rajan, and Tanaka, 2018; Tanaka, 2019), leading to the sum rule

$$M_N = M_m + M_A. \tag{20}$$

Current phenomenology (Hoferichter *et al.*, 2016) and lattice QCD calculations (Alexandrou, Bacchio *et al.*, 2020b) indicate that $M_m/M_N \approx 10\%$, suggesting that most of the proton mass comes from the trace anomaly (and hence from the gluons since γ_m is small). To clarify the actual meaning of this result, it was noted by Lorcé (2018a) that the sum rule (20) is equivalent to writing

$$M_N = \sum_a \int \mathrm{d}^3 r\, g_{\mu\nu} \mathcal{T}_a^{\mu\nu}(\vec{r}) = \sum_a (U_a - 3W_a). \tag{21}$$

While the total pressure-volume work vanishes owing to the virial theorem (14), it does nevertheless contribute to the separate quark and gluon contributions to the EMT trace. Since $\sum_q U_q$ and U_G turn out to be of the same order of magnitude, the smallness of M_m relative to M_A indicates in reality that $\sum_q W_q = -W_G > 0$. In other words, the net quark force is repulsive and is exactly balanced by the net attractive gluon force.

Since the four-momentum (and hence the mass) of a system is defined via the $T^{0\mu}$ components of the EMT, it was argued by Lorcé (2018a) and Lorcé *et al.* (2021) that a genuine mass decomposition should in principle not entail the components T^{ii}. In particular, the quantities $\bar{M}_g$ and M_A involve the gluon pressure-volume work W_g, and hence do not have a clean interpretation as mass contributions. From this point of view, Eqs. (17) and (20) should both instead be regarded as mere sum rules mixing the genuine mass decomposition (16) with the virial theorem (14).

E. Decomposition of proton spin

A similar discussion elucidates the proton spin decomposition. The total angular momentum (AM) operator is defined in terms of the Belinfante (symmetric) EMT $T^{\mu\nu}_{\mathrm{Bel}} = T^{\{\mu\nu\}}$ as

$$\mathcal{J}^i = \int \mathrm{d}^3 r\, \epsilon^{ijk} r^j T^{0k}_{\mathrm{Bel}}. \tag{22}$$

Because of the explicit factor of r^j, the expectation value of this operator in a momentum eigenstate turns out to be ill defined. A proper treatment requires the use of wave packets and amounts to considering matrix elements with nonvanishing momentum transfer (Bakker, Leader, and Trueman, 2004; Leader and Lorcé, 2014).

For convenience, only the longitudinal AM [i.e., the component along the proton average momentum $\vec{P} = (1/2)(\vec{p}' + \vec{p})$ defining the z direction] is considered here. The discussion of the transverse AM turns out to be much more complex because of its dependence on both $|\vec{P}|$ and the choice of origin; see Lorcé (2018b, 2021) and references therein. From the splitting of the EMT in Eq. (2), one finds that the quark and gluon contributions to the proton spin $\langle \mathcal{J}^z \rangle = \sum_q J_q^z + J_G^z$ are given by (Ji, 1997b)

$$J_a^z = J_a(0) \tag{23}$$

for a proton polarized in the z direction.

When one instead works with an asymmetric EMT, the quark AM operator can be further decomposed into orbital and intrinsic AM terms

$$\mathcal{J}_q^i = \int \mathrm{d}^3 r\, \epsilon^{ijk} r^j T_q^{0k} + \int \mathrm{d}^3 r\, \frac{1}{2} \bar{\psi}_q \gamma^i \gamma_5 \psi_q. \tag{24}$$

Calculating the corresponding matrix elements, one then finds that $J_q^z = L_q^z + S_q^z$, with

$$\begin{aligned} L_q^z &= J_q(0) - S_q(0), \\ \sum_q S_q^z &= \tfrac{1}{2}\Delta\Sigma. \end{aligned} \tag{25}$$

Combining the results of Eqs. (24) and (25) with the fact that the proton is a spin-1/2 particle, one arrives at the constraints given in Eqs. (6) and (7).

Since gluons are spin-1 particles, one wonders whether the gluon AM could also be decomposed into orbital and intrinsic contributions. This can be done, but it requires nonlocal operators to preserve gauge invariance (Chen *et al.*, 2008; Hatta, 2012; Lorcé, 2013a; Lorcé, 2013b; Leader and Lorcé, 2014; Wakamatsu, 2014). One is then led to the canonical (or Jaffe-Manohar) spin decomposition (Jaffe and Manohar, 1990), to be distinguished from the one derived here from the local EMT [Eq. (2)] and known as the kinetic (or Ji) spin decomposition (Ji, 1997b). Finally, it is possible to push this analysis further and study the spatial distribution of angular momentum (Lorcé, Mantovani, and Pasquini, 2018).

III. MEASURING GRAVITATIONAL FORM FACTORS

There is no direct way to measure the proton GFFs, as measurements of the graviton-proton interaction would be required (Kobzarev and Okun, 1962; Pagels, 1966). More recent theoretical developments have shown, however, that the GFFs may be probed indirectly in various exclusive processes. That is the subject of this section.

A. Deeply virtual Compton scattering

In deeply virtual Compton scattering (DVCS), the most explored process to date that accesses GFFs, high-energy charged leptons scatter off protons or nuclei by exchanging a deeply virtual photon, producing a real photon in the final state (Müller *et al.*, 1994; Radyushkin, 1996; Ji, 1997a). As in DIS (see Sec. I.C), in the high-energy limit defined by $Q^2 \to \infty$ and $P \cdot q \to \infty$, with $(-t) \ll Q^2$ and $P = (p' + p)/2$, the process is described in QCD (Collins and Freund, 1999) in terms of the upper part of the handbag diagram shown in Fig. 2(a), which can be calculated in perturbative QCD, and a lower part described in terms of generalized parton distributions (GPDs). GPDs are universal, i.e., the same nonperturbative functions enter the description of different hard exclusive reactions.

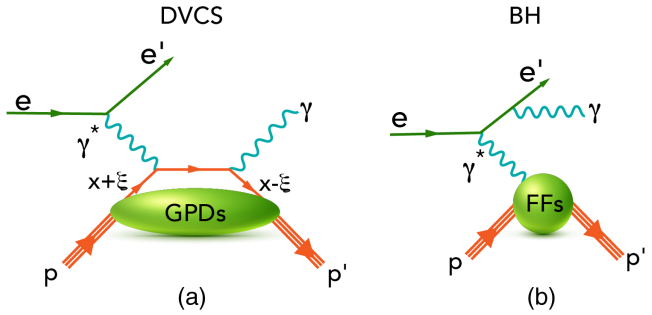

FIG. 2. (a) QCD factorization of the DVCS amplitude. The perturbatively calculable "hard part" is shown to lowest order in the strong coupling. The nonperturbative "soft part" is described by the universal quark GPDs. (b) One of the QED diagrams for the amplitude of the Bethe-Heitler process, which has the same final state as DVCS and interferes with it. The Bethe-Heitler process is calculable, with only the proton electromagnetic FFs required as input.

GPDs are functions of x, ξ, and t. The new quantity $\xi \approx x_B/(2-x_B)$ in the high-energy limit, called skewness, represents the longitudinal momentum transfer to the struck quark from the initial to final state; see Fig. 2(a). The variables ξ and t are observable in DVCS, while x is not observable and enters the DVCS amplitude as an integration variable. GPDs encompass both the PDFs and electromagnetic FFs discussed in Sec. I. For $p' \to p$ implying $\xi \to 0$ and $t \to 0$, GPDs reduce to PDFs; integrating the GPDs over x yields electromagnetic FFs.

GPDs parametrize the matrix elements of certain nonlocal operators that can be expanded in terms of a series of local operators with various J^{PC} quantum numbers. This includes operators with the quantum numbers of the graviton ($J=2$), so part of the information about how the proton would interact with a graviton is encoded within this tower. As the electromagnetic coupling to quarks is many orders of magnitude stronger than gravity, the DVCS process is an effective tool for probing the proton's gravitational properties. Gluon GPDs are accessible in DVCS only at higher orders in α_s.

The leading contribution to DVCS is described in terms of four GPDs. Two of them, namely, $H_q(x,\xi,t)$ and $E_q(x,\xi,t)$, give access to the quark GFFs as follows:

$$\int_{-1}^{1} \mathrm{d}x\, x H_q(x,\xi,t) = A_q(t) + \xi^2 D_q(t),$$
$$\int_{-1}^{1} \mathrm{d}x\, x E_q(x,\xi,t) = B_q(t) - \xi^2 D_q(t), \tag{26}$$

where $B_q(t) = 2J_q(t) - A_q(t)$ is the quark contribution to the proton's anomalous gravitomagnetic moment. Analogous relations hold for gluons, and $B(0) = \sum_a B_a(0)$ vanishes due to Eqs. (5) and (6) (Kobzarev and Okun, 1962; Teryaev, 1999; Brodsky *et al.*, 2001; Lowdon, Chiu, and Brodsky, 2017; Cotogno, Lorcé, and Lowdon, 2019; Lorcé and Lowdon, 2020).

The actual observables in DVCS are Compton form factors (CFFs), which are expressed by means of factorization formulas in terms of complex-valued convolution integrals given, at leading order α_s, by

$$\mathrm{Re}\mathcal{H}(\xi,t) + i\mathrm{Im}\mathcal{H}(\xi,t) = \sum_q e_q^2 \int_{-1}^{1} \mathrm{d}x \left[\frac{1}{\xi - x - i\epsilon} - \frac{1}{\xi + x - i\epsilon}\right] H_q(x,\xi,t). \tag{27}$$

CFFs of other GPDs are defined similarly. The CFFs are related to measurable quantities such as differential cross sections and beam and target polarization asymmetries.

The DVCS cross section is typically small. Note that DVCS interferes with the Bethe-Heitler process [see Fig. 2(b)], which can be computed in QED given the proton's electromagnetic FFs, and has the same final state but with the final-state photon emitted from the electron lines. The interference term of the DVCS and Bethe-Heitler amplitudes provides access to $\mathrm{Im}\mathcal{H}(\xi,t)$ when a spin-polarized electron beam is employed, while $\mathrm{Re}\mathcal{H}(\xi,t)$ contributes dominantly to the unpolarized DVCS cross section and can be constrained through precise unpolarized cross-section measurements.

Convolution integrals like Eq. (27) cannot be inverted in a model-independent way to yield GPDs (Bertone *et al.*, 2021). However, with experimental information from other exclusive processes becoming available (as later discussed), the GPDs can be further constrained. Presently a model-independent extraction of the GPDs and, via Eq. (26), of the GFFs $A_q(t)$ and $J_q(t)$ is not possible. In the case of the GFF $D_q(t)$, however, the situation is more fortunate. In particular, the real and imaginary parts of $\mathcal{H}(\xi,t)$ are related by the fixed-t dispersion relation (Diehl and Ivanov, 2007; Anikin and Teryaev, 2008)

$$\mathrm{Re}\mathcal{H}(\xi,t) = \mathcal{C}_{\mathcal{H}}(t) + \frac{1}{\pi}\mathrm{P.V.}\int_0^1 \mathrm{d}\xi' \left[\frac{1}{\xi-\xi'} - \frac{1}{\xi+\xi'}\right]\mathrm{Im}\mathcal{H}(\xi',t), \tag{28}$$

where P.V. denotes the Cauchy principal value of the integral. Equation (28) contains a real subtraction term $\mathcal{C}_{\mathcal{H}}(t)$ given by

$$\mathcal{C}_{\mathcal{H}}(t) = 2\sum_q e_q^2 \int_{-1}^{1} \mathrm{d}z \frac{D^q_{\mathrm{term}}(z,t)}{1-z}, \tag{29}$$

where $D^q_{\mathrm{term}}(z,t)$, which was introduced by Polyakov and Weiss (1999) and further elucidated by Teryaev (2001), has the expansion (Goeke, Polyakov, and Vanderhaeghen, 2001)

$$D^q_{\mathrm{term}}(z,t) = (1-z^2)\sum_{\mathrm{odd}\, n} d^q_n(t) C_n^{3/2}(z), \tag{30}$$

with $C_n^{\alpha}(z)$ the Gegenbauer polynomials which diagonalize the leading-order evolution equations (the renormalization-scale dependence is not indicated in this Colloquium). In the limit of the renormalization scale $\mu \to \infty$, all $d^q_n(t)$ go to zero except $d^q_1(t)$, which is related to the GFF $D_q(t)$ as follows:

$$D_q(t) = \tfrac{4}{5} d^q_1(t) = \int_{-1}^{1} \mathrm{d}z\, z D^q_{\mathrm{term}}(z,t). \tag{31}$$

Thus, extracting information on $\mathrm{Im}\mathcal{H}(\xi,t)$ and $\mathrm{Re}\mathcal{H}(\xi,t)$ and their scale dependence from experimental data provides access to the GFF $D_q(t)$.

B. DVCS with positron and electron beams

When data with both positron and electron beams are available, it is possible to measure the beam charge asymmetry A_C, defined as the difference in the $ep \to ep\gamma$ cross section when it is measured with an electron beam and with a positron beam, divided by their sum

$$A_C = \frac{\sigma^{e^-} - \sigma^{e^+}}{\sigma^{e^-} + \sigma^{e^+}}. \tag{32}$$

The numerator of A_C is given by the real part of the DVCS and Bethe-Heitler interference term providing the cleanest access to $\mathrm{Re}\mathcal{H}$ (Kivel, Polyakov, and Vanderhaeghen, 2001; Belitsky, Müller, and Kirchner, 2002). In contrast, in DVCS measured with electrons (or positrons) alone additional theoretical assumptions in the CFF extraction procedure are unavoidable (Burkert *et al.*, 2021).

C. $\gamma\gamma^* \to \pi^0\pi^0$

The process $\gamma\gamma^* \to \pi^0\pi^0$ shown in Fig. 3(a) can be studied at, for instance, electron-positron colliders and is described in terms of generalized distribution amplitudes that correspond to GPDs continued analytically from the t to the s channel (Müller *et al.*, 1994; Diehl *et al.*, 1998). In this way, one can access information on GFFs in the timelike region where $t > 0$ (Kumano, Song, and Teryaev, 2018; Lorcé, Pire, and Song, 2022). This process provides a unique opportunity to study the structure of unstable hadrons like pions that are not available as targets.

D. Timelike Compton scattering and double DVCS

Several other processes provide complementary information about the nucleon GFFs. One of them is timelike Compton scattering (TCS), $\gamma p \to p'\gamma^*$, where the final-state virtual photon produces an e^+e^- pair (Berger, Diehl, and Pire, 2002; Pire, Szymanowski, and Wagner, 2011; Chatagnon *et al.*, 2021). In TCS, $\mathrm{Im}\mathcal{H}$ can be accessed through the polarized beam-spin asymmetry and $\mathrm{Re}\mathcal{H}$ through a forward-backward asymmetry of the final-state e^+e^- pair in its center-of-mass frame.

The double DVCS process (Belitsky and Müller, 2003; Guidal and Vanderhaeghen, 2003) displayed in Fig. 4(a) may also play an important role at future facilities. It is a variant of DVCS with the final-state timelike photon converting into a e^+e^- or $\mu^+\mu^-$ pair. While in DVCS the GPDs are sampled along the lines $x = \pm\xi$ in the convolution integrals (27), this constraint is relaxed in double DVCS due to the variable invariant mass of the lepton pair. This is an advantage of this process and will be of importance for less model-dependent global extractions of GPDs.

E. Meson production

Deeply virtual meson production (Collins, Frankfurt, and Strikman, 1997) is another process sensitive to GPDs; see Fig. 4(b). Production of different vector mesons provides sensitivity to GPDs of different quark flavors, which is an advantage over DVCS. However, this process is more difficult to analyze than DVCS since gluons contribute on the same footing as quarks [Fig. 4(b) shows only a quark diagram], and one in general expects larger power corrections. In addition, the process of heavy vector quarkonium photoproduction was shown to factorize in the heavy quark limit at one-loop order in perturbative QCD (Ivanov *et al.*, 2004).

Exclusive J/Ψ photoproduction at threshold is expected to be sensitive to gluon GFFs (Kharzeev, 1996, 2021) and more generally, as depicted in Fig. 3(b), to gluon GPDs (Hatta and Yang, 2018; Guo, Ji, and Liu, 2021), which in DVCS are accessible only at higher orders in α_s.

Gluon GFFs were recently extracted from this process by Duran *et al.* (2023), but the link with the physical observables is not direct and requires approximations (Sun, Tong, and Yuan, 2021, 2022). J/Ψ photoproduction can also be studied with quasireal photons of virtualities as low as $Q^2 \lesssim 0.1$ GeV^2 emitted by electrons, together with electroproduction and DVCS.

Finally, a new class of hard scattering processes with multiparticle final states has recently emerged (Ivanov *et al.*, 2002; Boussarie *et al.*, 2017; Duplančić *et al.*, 2018; Pedrak *et al.*, 2020; Grocholski *et al.*, 2022; Qiu and Yu, 2022). Those reactions are theoretically appealing, but measuring them is challenging.

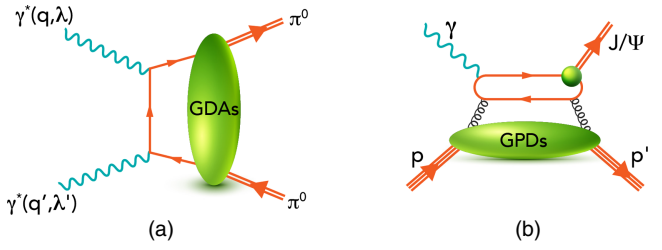

FIG. 3. (a) The process $\gamma\gamma^* \to \pi^0\pi^0$ is described in terms of generalized distribution amplitudes, which provide access to GFFs in the timelike region $t > 0$. (b) Threshold J/Ψ photoproduction on the proton. This process is sensitive to the gluon GPDs.

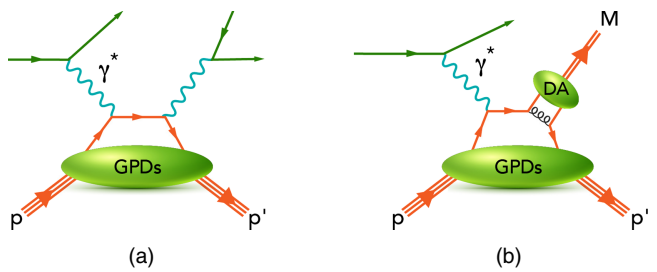

FIG. 4. (a) The leading double DVCS diagram and (b) one of the leading diagrams for deeply virtual meson production. The ellipse where the meson (M) is produced is the nonperturbative distribution amplitude (DA).

The relatively new progress reviewed here paved the way for interesting and even more recent experimental developments, which is reviewed in Sec. V with a focus on DVCS and TCS. Section IV is devoted to the theory of GFFs, whose history is equally interesting and began much earlier.

IV. THEORETICAL RESULTS

GFFs were introduced by Kobzarev and Okun (1962), who considered spin-0 and spin-1/2 particles and parity-violating weak effects (not discussed here), proved the vanishing of proton's anomalous gravitomagnetic moment $B(0) = 0$, and showed that one would need energies around the Planck scale to measure GFFs in gravitational interactions. This section presents an overview of GFFs from the theoretical perspective with a particular focus on $D(t)$, the least known of the total GFFs. Despite the focus on the proton, it is insightful to mention other hadrons for comparison when appropriate.

A. Chiral symmetry and the *D*-term of the pion

GFFs received little attention from the community until it was realized that matrix elements such as $\langle \pi, \pi | T^{\mu\nu} | 0 \rangle$ enter the QCD description of hadronic decays of charmonia (Voloshin and Zakharov, 1980; Novikov and Shifman, 1981) or the decay of a hypothetical light Higgs boson, an idea entertained in the early 1990s, when the possibility of a light Higgs was not yet experimentally excluded (Donoghue, Gasser, and Leutwyler, 1990). These matrix elements are related to pion GFFs in the timelike region $t > 0$.

In general, hadronic EMT matrix elements cannot be computed analytically in QCD, but the pion is a notable exception. The QCD Lagrangian (1) exhibits a classical symmetry under global left- and right-handed rotations in the flavor space of up, down, and strange quarks. This symmetry is approximate due to the small but nonzero quark masses m_q. If this symmetry were realized in nature, then, for example, the nucleon state $N(940)$ (here N stands for a state with nucleon isopin quantum number and the number in parentheses is the rounded mass of the state in GeV/c^2) with the spin-parity quantum numbers $J^P = (1/2)^+$ should have the same mass as its negative-parity partner $N(1535)$, with $J^P = (1/2)^-$ modulo small corrections due to the small m_q. However, the latter is almost 600 MeV/c^2 heavier than the nucleon, an effect that cannot be attributed to current quark mass effects. The phenomenon in which a symmetry of the Lagrangian is not realized in the particle spectrum is known as spontaneous symmetry breaking (Nambu and Jona-Lasinio, 1961a, 1961b). It is accompanied by the emergence of massless Goldstone bosons, corresponding in QCD to pions, kaons, and η mesons, which are not massless but are light compared to other hadrons.

In theoretical calculations, chiral symmetry is a powerful tool allowing one to evaluate the matrix elements of Goldstone bosons in the chiral limit (and for $t \to 0$). In this way, one obtains for the pion (and kaon and η) D-term (Novikov and Shifman, 1981)

$$\lim_{m_\pi \to 0} D_\pi = -1. \tag{33}$$

Deviations from the chiral limit are systematically calculable in chiral perturbation theory (Donoghue and Leutwyler, 1991) and are expected to be small for pions and more sizable for kaons and the η meson (Hudson and Schweitzer, 2017). The relation between the stability of the pion and spontaneous chiral symmetry breaking was discussed by Son and Kim (2014), and the gravitational interactions of Goldstone bosons were studied by Voloshin and Dolgov (1982) and Leutwyler and Shifman (1989). For hadrons other than pions, the techniques based on the chiral limit of QCD cannot predict the D-term, but they can still be explored to provide insights on some properties of $D(t)$, as discussed in Sec. IV.C.

B. GFFs in model studies

Interest in GFFs was once again renewed after it was shown that they can be inferred from hard exclusive reactions via GPDs and play a key role for the understanding of the mass and spin structure of the proton (see Sec. II). Interest was further stimulated by their interpretation in terms of forces inside hadrons (Polyakov, 2003). The first model study of proton GFFs was presented by Ji, Melnitchouk, and Song (1997) for the bag model, followed by work using the chiral quark-soliton model (Petrov *et al.*, 1998; Schweitzer, Boffi, and Radici, 2002; Ossmann *et al.*, 2005; Goeke, Grabis, Ossmann, Polyakov *et al.*, 2007; Goeke, Grabis, Ossmann, Schweitzer *et al.*, 2007; Wakamatsu, 2007; Kim and Kim, 2021) and Skyrme models (Cebulla *et al.*, 2007; Jung, Yakhshiev, and Kim, 2014; Perevalova, Polyakov, and Schweitzer, 2016).

Extensive GFF model studies for the nucleon and other hadrons were presented in light-front constituent quark models (Pasquini and Boffi, 2007; Sun and Dong, 2020), diquark approaches (Hwang and Müller, 2008; Kumar, Mondal, and Sharma, 2017; Chakrabarti *et al.*, 2020; Choudhary *et al.*, 2022; Fu, Sun, and Dong, 2022; Amor-Quiroz *et al.*, 2023), holographic AdS/QCD models (Abidin and Carlson, 2008, 2009; Brodsky and Teramond, 2008; Chakrabarti, Mondal, and Mukherjee, 2015; Mondal, 2016; Mondal *et al.*, 2016; Mamo and Zahed, 2020, 2021, 2022; Fujita *et al.*, 2022), a large-N_c bag model (Neubelt *et al.*, 2020; Lorcé, Schweitzer, and Tezgin, 2022), a cloudy bag model (Owa, Thomas, and Wang, 2022), light-cone QCD sum rules (Anikin, 2019; Azizi and Özdem, 2020; Özdem and Azizi, 2020; Aliev, Şimşek, and Barakat, 2021; Azizi and Özdem, 2021), the Nambu–Jona-Lasinio model (Freese and Cloët, 2019), a chiral quark-soliton model with strange and heavier quarks (Kim *et al.*, 2021; Won, Kim, and Kim, 2022; Ghim *et al.*, 2023), a dual model with complex Regge trajectories (Fiore, Jenkovszky, and Oleksiienko, 2021), and an instant-form relativistic impulse approximation approach (Krutov and Troitsky, 2021, 2022). Algebraic GPD *Ansätze* were used to shed light on pion and kaon GFFs (Raya *et al.*, 2022), and toy models (Kim *et al.*, 2023) as well as light-cone convolution models (Freese and Cosyn, 2022a) were used to study the deuteron GFFs.

The D-terms of nuclei were studied in the liquid-drop model (Polyakov, 2003), which revealed that for nuclei $D(0) \propto A^{7/3}$ grows strongly with mass number A. Studies in the Walecka model (Guzey and Siddikov, 2006) supported

this prediction, which can be tested in DVCS experiments with nuclear targets. Different results were obtained in a nonrelativistic nuclear spectral function approach (Liuti and Taneja, 2005). Nuclear GFFs were also investigated in Skyrme model frameworks (Kim, Schweitzer, and Yakhshiev, 2012; Jung *et al.*, 2014; Kim, Yakhshiev, and Kim, 2022; García Martín-Caro, Huidobro, and Hatta, 2023).

The GFFs for a constituent quark were studied in a light-front Hamiltonian approach (More *et al.*, 2022, 2023) that, after rescaling and regularization of infrared divergences, reproduced QED results for an electron (Metz, Pasquini, and Rodini, 2021; Freese *et al.*, 2023). GFFs of the photon in QED were studied by Friot, Pire, and Szymanowski (2007), Gabdrakhmanov and Teryaev (2012), Polyakov and Sun (2019), and Freese and Cosyn (2022b). An insightful model for composite particles is the Q-ball system, where stable, metastable, and unstable states were investigated, showing that, among all studied particle properties, $D(0)$ is the most sensitive to details of the dynamics (Mai and Schweitzer, 2012a, 2012b; Cantara, Mai, and Schweitzer, 2016). Notably the same conclusions were obtained in the bag model, where for the Nth highly excited nucleon state the mass increases as $M \propto N^3$, whereas $D(0) \propto N^8$ grows much more strongly with N (Neubelt *et al.*, 2020).

C. Limits in QCD and dispersion relations

Model-independent results for GFFs can be obtained in certain limiting situations in QCD, such as when the number of colors $N_c \to \infty$ or when $|t|$ becomes small or large, and through the use of dispersion relation. These methods are complementary to the nonperturbative lattice QCD methods that are reviewed in Sec. IV.D.

In the large-N_c limit of QCD, baryons are described as solitons of mesonic fields (Witten, 1979). Large-N_c QCD has not been solved (in $3+1$ dimensions), and the soliton field is not known (though it can be modeled). Nontrivial results can, however, be derived based on the known symmetries of the large-N_c soliton field, which are generally well supported in nature (Dashen, Jenkins, and Manohar, 1994) despite $N_c = 3$. The relations of the GFFs of the nucleon and Δ were studied in the large-N_c limit of QCD by Panteleeva and Polyakov (2020). The GFFs of the Δ are difficult to measure, but such relations can be tested, for instance, in soliton models like the chiral quark-soliton model or Skyrme model (mentioned in Sec. IV.B) or in lattice QCD, which is discussed in Sec. IV.D.

At small $|t|$, one can use chiral perturbation theory, where one writes an effective Lagrangian in terms of hadronic degrees of freedom with the most general interactions allowed by chiral symmetry, and free parameters that can be inferred from comparisons of observable quantities to experiments. A pioneering study to lowest order in chiral perturbation theory was presented by Belitsky and Ji (2002), and studies at next-to-leading order (Diehl, Manashov, and Schäfer, 2006) were completed by Alharazin *et al.* (2020). In this way, one can obtain valuable model-independent information on the t dependence of GFFs for small t. For instance, for the nucleon the slope of $D(t)$ at $t = 0$ diverges in the chiral limit as

$$\left.\frac{\mathrm{d}}{\mathrm{d}t} D(t)\right|_{t=0} = -\frac{g_A^2 M_N}{40\pi f_\pi^2 m_\pi} + \cdots, \tag{34}$$

where $g_A = 1.26$ is the isovector axial constant, $f_\pi = 93$ MeV is the pion decay constant, m_π is the pion mass, and the dots indicate finite higher-order chiral corrections. These results are reproduced in chiral soliton models (Cebulla *et al.*, 2007; Goeke, Grabis, Ossmann, Polyakov *et al.*, 2007). The value of the D-term cannot be determined exactly in chiral perturbation theory for hadrons other than Goldstone bosons. It is, however, possible to derive an upper bound, for instance, for the nucleon $\mathrm{D}/M_N \leq -(1.1 \pm 0.1)\ \mathrm{GeV}^{-1}$ in the chiral limit (Gegelia and Polyakov, 2021). The GFFs of the ρ meson (Epelbaum *et al.*, 2022) and Δ resonance (Alharazin *et al.*, 2022) have also been studied in chiral perturbation theory.

Model-independent results for GFFs can also be derived for asymptotically large momentum transfers using power counting and perturbative QCD methods (Tanaka, 2018; Tong, Ma, and Yuan, 2022, 2021). For instance, the proton GFFs $A_a(t)$ for quarks and gluons behave like $1/t^2$ at large $(-t) \to \infty$. Since QCD factorization of hard exclusive processes requires $(-t) \ll Q^2$ and Q^2 is in practice often not large in current experimental settings, such results provide important theoretical guidelines to extrapolate to larger $|t|$. However, based on experience with analogous perturbative QCD predictions for the electromagnetic pion form factor [see Horn and Roberts (2016) for a review], it is difficult to anticipate how large the momentum transfer t must be for a form factor to reach the asymptotic regime.

A theoretical study of the quark contribution to the nucleon GFF $D_q(t)$ in the range $0 < (-t) < 1\ \mathrm{GeV}^2$ was presented by Pasquini, Polyakov, and Vanderhaeghen (2014) based on dispersion theory methods that rely on general principles like relativity, causality, and unitarity. This approach does not require modeling other than making use of available information on pion-nucleon partial-wave helicity amplitudes and relying on mild assumptions like the saturation of the t-channel unitarity relation in terms of the two-pion intermediate states or input pion PDF parametrizations.

D. Lattice QCD

Complementing the insights gained from models of the proton and nuclear structure, numerical lattice QCD calculations give direct and controllable QCD predictions for matrix elements of the EMT operator. In particular, lattice QCD is the only known systematically improvable approach to computing observables in QCD in the low-energy (nonperturbative) regime. The approach proceeds via a discretization of the QCD Lagrangian (1) onto a Euclidean spacetime lattice, with a finite lattice spacing that is not physical but that acts as a method of regularization of the theory. Calculations then proceed via Monte Carlo integration of the high-dimensional discretized path integral; continuum QCD results are recovered in the limit of vanishing lattice discretization scale, infinite lattice volume, and precise matching of the bare quark masses to reproduce simple physical observables. Using this approach, matrix elements of local operators, such as the

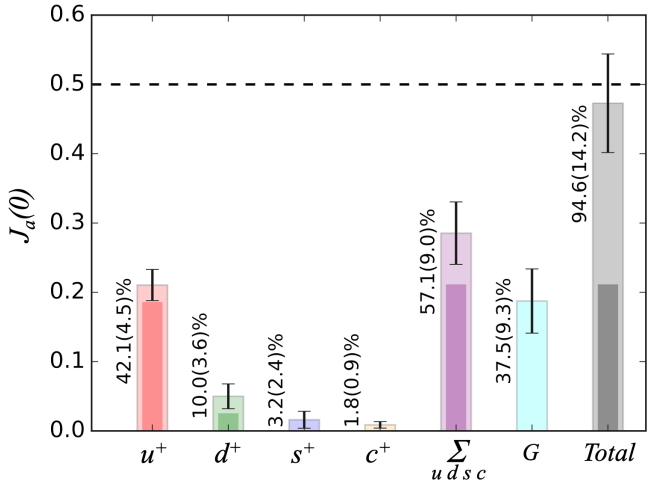

FIG. 5. Proton spin decomposition computed in lattice QCD by Alexandrou, Bacchio *et al.* (2020a) given in the $\overline{\text{MS}}$ scheme at 2 GeV. Each component includes the contribution of both the quarks and the antiquarks ($q^+ = q + \bar{q}$). Outer (light) [inner (dark)] shaded bars denote the total (purely connected) contributions.

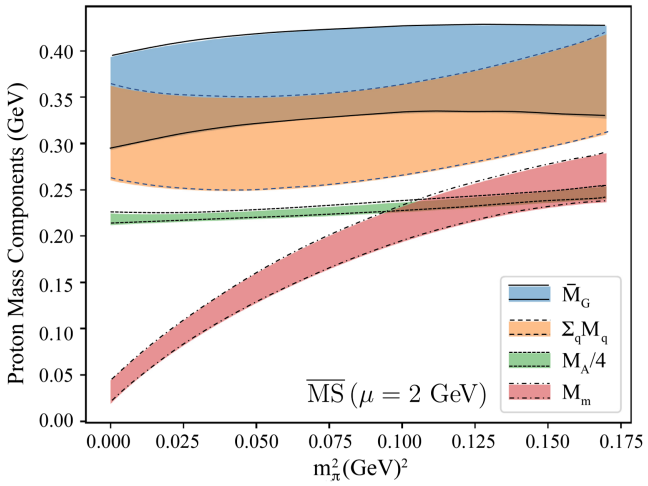

FIG. 6. Ji's mass decomposition [i.e., the combination of Eqs. (16) and (17)] for a proton computed in lattice QCD by Yang, Liang *et al.* (2018) at a scale $\mu = 2$ GeV as a function of the pion mass.

separated quark and gluon components of the EMT in proton or nuclear states, can be computed directly.

In the current era of precision lattice QCD calculations of proton structure, particular efforts have been made to determine the complete decomposition of the proton's spin and momentum into individual quark and gluon contributions with high precision and systematic control. For example, recent lattice QCD studies have isolated all angular momentum components in the kinetic (or Ji) decomposition (Alexandrou, Bacchio *et al.*, 2020a; Wang *et al.*, 2022), with ≈10% uncertainty in the total quark and gluon contributions; the results from one collaboration are shown in Fig. 5. This example illustrates the complementarity between theory and experiment in this area; flavor separation in lattice QCD calculations is in principle more straightforward, although some contributions, such as those from gluons or those arising from "disconnected" contributions, for instance, strange and charm quarks in the proton, are difficult to compute because of signal-to-noise challenges. Computing the gluon spin and orbital angular momentum in the Jaffe-Manohar decomposition introduces additional challenges to the lattice QCD approach, but first results have been achieved based on constructions using both local and nonlocal operators (Yang *et al.*, 2017; Engelhardt *et al.*, 2020).

In the same vein, precise decompositions of the quark and gluon contributions to the proton's momentum, which are related to the mass decomposition, have been achieved with complete systematic control in the same computational frameworks that yielded the spin decomposition (Alexandrou, Bacchio *et al.*, 2020a; Wang *et al.*, 2022). Contributions from the trace anomaly to the proton's mass decomposition are more difficult to compute directly with systematic control but have been constrained using the trace sum rule (20). Figure 6 shows the first insight from lattice QCD into the pion mass (or quark mass) dependence of the proton's mass decomposition (Yang, Liang *et al.*, 2018). It is particularly notable that, while the quark scalar condensate contribution varies rapidly with quark mass, the other contributions, including that of the trace anomaly, remain approximately constant.

While local matrix elements in nuclear states can in principle be computed in lattice QCD in the same way as in the proton state, such calculations face significant practical and computational challenges, in particular, compounding factorial and exponential growth in computational cost with the atomic number of the nuclear state. To date a single first-principles calculation of isovector quark momentum fraction $A_{u-d}(0)$ in ^{3}He (Detmold, Illa *et al.*, 2021) has been achieved; despite significant systematic uncertainties, including this lattice result as a constraint in global fits of experimental lepton-nucleus scattering data yields improved constraints on the nuclear parton distributions. Over the coming decade, one can anticipate that the control and precision achieved in first-principles calculations of simple aspects of the gravitational structure of the proton will be extended to nuclear states.

In addition to forward-limit matrix elements, lattice QCD has also been used to compute the quark and gluon GFFs of the proton and other hadrons. Such calculations are computationally more demanding than those needed to constrain the forward-limit components, and statistical uncertainties increase with $|t|$. As a result, these studies have not yet achieved the same level of systematic control as the spin and mass decomposition. Nevertheless, the quark contributions to the proton's GFFs (and those of other hadrons such as the pion) have been computed with $|t| \lesssim 1$ GeV^2 (Brömmel *et al.*, 2006, 2007; Hägler *et al.*, 2008; Bali *et al.*, 2016; Alexandrou *et al.*, 2017, 2018, 2020; Yang, Gong *et al.*, 2018; Yang, Liang *et al.*, 2018; Alexandrou, Bacchio *et al.*, 2020a). The gluon contributions to the proton's GFFs are far less well constrained, and almost all calculations to date have been performed with quark masses corresponding to larger-than-physical values of the pion mass (Detmold, Pefkou, and Shanahan, 2017; Shanahan and Detmold, 2019a, 2019b; Pefkou, Hackett, and Shanahan, 2022). Nevertheless, the

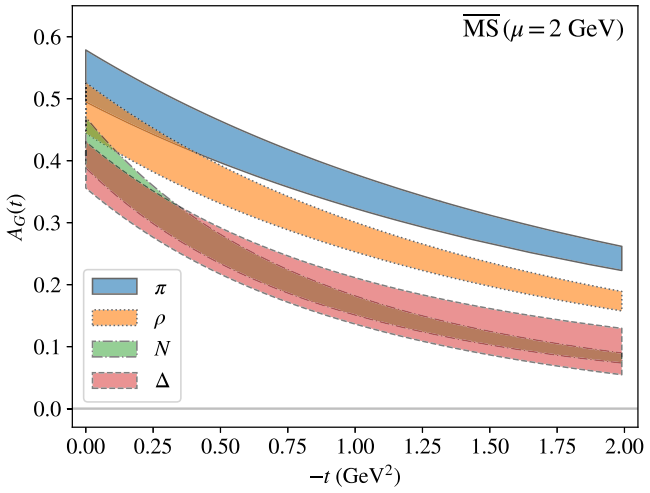

FIG. 7. $A_G(t)$ GFF for various hadrons discussed by Pefkou, Hackett, and Shanahan (2022), with quark masses corresponding to a larger-than-physical value of the pion mass of 450 MeV.

gluon GFFs with $|t| \lesssim 2\ \text{GeV}^2$ were computed for a range of hadrons by Pefkou, Hackett, and Shanahan (2022), allowing qualitative comparisons of their t dependence, as illustrated in Fig. 7. Of particular recent interest has been the $D(t)$ GFF, which does not have a sum-rule constraint in the foward limit; a comparison between lattice QCD calculations of the quark and gluon contributions is illustrated in Fig. 8.

In contrast to local matrix elements, matrix elements defined with light-cone separations, yielding, for instance, the x dependence of GPDs, cannot be directly computed in Euclidean spacetime but must instead be approached by indirect means. Significant developments over the last two decades have yielded a range of complementary approaches to direct calculations of GPDs themselves in the lattice QCD framework (Detmold and David Lin, 2006; Ji, 2013; Chambers *et al.*, 2017; Radyushkin, 2017; Ma and Qiu, 2018; Constantinou *et al.*, 2021; Detmold, Grebe *et al.*, 2021). Given the significant technical and computational challenges of these approaches, the first lattice QCD studies of the x dependence of the proton GPDs were achieved only in

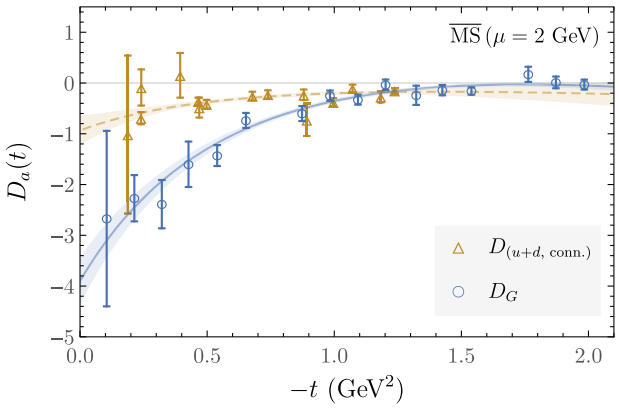

FIG. 8. $D_G(t)$ and $D_{u+d}(t)$ GFF for the proton as discussed by Shanahan and Detmold (2019a) and Hägler *et al.* (2008), respectively, with quark masses corresponding to a pion mass of approximately 450 MeV.

2020 (Alexandrou, Cichy *et al.*, 2020; Lin, 2021). Calculations with complete systematic control will require continuing effort in the coming years.

V. EXPERIMENTAL RESULTS

This section presents a discussion of the DVCS data and the analysis procedure that led to the first extraction of the proton D-term form factor $D_q(t)$ from data collected with the CLAS detector at Jefferson Lab (JLab). The extraction of $D_q(t)$ of π^0 from Belle data and other phenomenological results are also reviewed.

A. DVCS in fixed-target and collider experiments

The first measurements of DVCS on unpolarized protons were carried out with the H1 (Adloff *et al.*, 2001) experiment and later with the ZEUS (Chekanov *et al.*, 2003) experiment, both at the HERA collider. The first observation of the $\sin(\phi)$ dependence for the $\vec{e}p \to e'p'\gamma$ process as a signature of the interference of the DVCS and Bethe-Heitler amplitudes came from the CLAS (Stepanyan *et al.*, 2001) and HERMES detectors (Airapetian *et al.*, 2001).

These initial results triggered the development of a worldwide dedicated experimental program to measure the DVCS process with high precision and in a large kinematic range with HERMES at HERA, Hall A and CLAS at JLab, and COMPASS at CERN. A review of the early DVCS experiments was given by d'Hose, Niccolai, and Rostomyan (2016).

B. First extraction of the proton GFF $D_q(t)$

In this section, the data and procedure used by Burkert, Elouadrhiri, and Girod (2018) to obtain the first determination of the quark contribution to the D-term of the proton are described. This work is based on two main pieces of experimental information from the CLAS detector at JLab (Mecking *et al.*, 2003), namely, the beam-spin asymmetry (BSA) measured with spin-polarized electron beams and the unpolarized cross section for DVCS on the proton.

The polarization asymmetries and differential cross sections have been used to extract the imaginary and real parts of the CFF $\mathcal{H}$, respectively. Using the dispersion relation technique to determine the subtraction term $\mathcal{C}_{\mathcal{H}}(t)$, as discussed in Sec. III.A, requires the full integral over $0 \le \xi \le 1$ at fixed t to be evaluated. As this process requires extrapolations to both $\xi = 0$ and 1 that are unreachable in experiments, a parametrization of the ξ dependence of $\text{Im}\mathcal{H}$ close to these limits has been incorporated to fit the data.

In the first step, fits of the BSA (Girod *et al.*, 2008) and of the unpolarized differential cross sections (Jo *et al.*, 2015) for DVCS were performed to estimate $\text{Im}\mathcal{H}(\xi, t)$ and $\text{Re}\mathcal{H}(\xi, t)$ at fixed kinematics in ξ and t in the ranges covered by the data. The BSA is defined as

$$A_{LU}(\xi, t) = \frac{N^+(\xi, t) - N^-(\xi, t)}{N^+(\xi, t) + N^-(\xi, t)}, \tag{35}$$

where N^+ and N^- refer to the measured event rates at electron helicities $+1$ and -1, respectively.

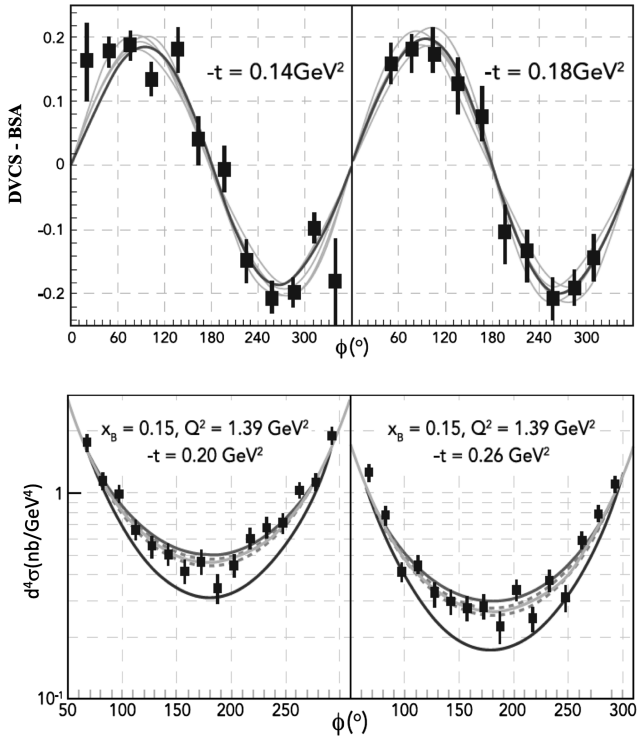

FIG. 9. Top panels: the expected $\sin\phi$ dependence is fit to the data. The thick solid lines are the global fits using the parametrization according to Eq. (36). The bunched thin solid lines represent local fits. The spread of the lines represents estimates of the systematic uncertainties. Bottom panels: the unpolarized cross section at fixed ξ and Q^2 for different t values. The azimuthal ϕ angle dependence of the cross section is fit to the experimental data. The thin dark solid line is the global fit. The upper thin gray lines represent fits at the given kinematics, with the dashed lines showing the systematic uncertainties. The lower thick black lines show the Bethe-Heitler contributions. Note the logarithmic vertical scale. Adapted from Burkert, Elouadrhiri, and Girod, 2018.

The experimentally measured BSA in $\vec{e}p \to ep\gamma$ contains not only the DVCS term with the photon generated at the proton vertex but also the Bethe-Heitler term with the photon generated at the incoming or scattered electron; see Fig. 2. Both have the same final state and thus interfere. They generate a $\sin\phi$-dependent interference contribution, as seen in Fig. 9. The DVCS term is dominated by the CFF $\mathrm{Im}\mathcal{H}$ and the Bethe-Heitler term is real and is given by the elastic electromagnetic FFs.

Note that this analysis does not rely on extracted cross sections but rather on asymmetries of event rates in specific bins. This is an essential advantage, as it avoids accounting for systematic uncertainties that must be included in the cross-section extraction. The uncertainties in $A_{LU}(\xi,t)$ are dominated by statistics rather than systematic uncertainties, which determines the local values of $\mathrm{Im}\mathcal{H}$ precisely, as seen in the top panels of Fig. 9, which show the BSA and the differential cross sections for selected kinematic bins.

In the second step, the $\mathrm{Im}\mathcal{H}(\xi,t)$ are fit with the functional form used in global fits (Müller *et al.*, 2014; Kumerički, Liuti, and Moutarde, 2016), with the parameters fit to the local CLAS data. The imaginary part is written as

$$\mathrm{Im}\mathcal{H}(\xi,t) = \frac{\mathcal{N}}{1+\xi}\frac{[2\xi/(1+\xi)]^{-\alpha(t)}[(1-\xi)/(1+\xi)]^{b}}{\{1-[(1-\xi)/(1+\xi)]t/M^2\}^{p}}, \quad (36)$$

where $\mathcal{N}$ is a free normalization constant, $\alpha(t)$ is fixed from small-x Regge phenomenology as $\alpha(t) = 0.43 - 0.85t$ GeV^{-2}, b is a free parameter controlling the large-x behavior, p is fixed at 1 for the valence quarks, and M is a free parameter controlling the t dependence.

The real and imaginary parts are fit together, including the subtraction term in the dispersion relation (28). Figure 10 compares the fits at fixed kinematics (local fits) with the global fit for one of the t values. The global and local fits show good agreement in ξ and t kinematics where they overlap.

In the fit, $\mathcal{C}_{\mathcal{H}}(t)$ is obtained at fixed t. The results for the subtraction term and the fit to the multipole form

$$\mathcal{C}_{\mathcal{H}}(t) = \mathcal{C}_{\mathcal{H}}(0)\left[1 - \frac{t}{M^2}\right]^{-\lambda} \quad (37)$$

are displayed in Fig. 11, where $\mathcal{C}_{\mathcal{H}}(0)$, λ, and M^2 are the fit parameters, with their values found to be

$$\begin{aligned} \mathcal{C}_{\mathcal{H}}(0) &= -2.27 \pm 0.16 \pm 0.36, \\ M^2 &= 1.02 \pm 0.13 \pm 0.21 \text{ GeV}^2, \\ \lambda &= 2.76 \pm 0.23 \pm 0.48. \end{aligned} \quad (38)$$

The first error in Eq. (38) is the fit uncertainty and the second error is due to the systematic uncertainties. When the fit errors for $\mathcal{C}_{\mathcal{H}}(0)$ and the systematic errors in quadrature $\sigma_{\mathcal{C}_{\mathcal{H}}(0)} = \sqrt{0.16^2 + 0.36^2} \approx 0.39$ are added, the significance S of the knowledge of the subtraction term is

$$S = \frac{\mathcal{C}_{\mathcal{H}}(0)}{\sigma_{\mathcal{C}_{\mathcal{H}}(0)}} \approx 5.8. \quad (39)$$

More flexible analyses based on unconstrained artificial neural network techniques (Kumerički, 2019; Dutrieux *et al.*, 2021) find, however, that a more conservative extraction of the subtraction constant from the currently available experimental data remains compatible with zero within large uncertainties.

In the analysis of Burkert, Elouadrhiri, and Girod (2018), the term $d_3^q(t)$ and other higher-order terms have been omitted in the expansion (30) to extract the GFF $D_q(t)$. The estimated effect is included in the systematic error analysis. It is also assumed that u and d quarks have the same first moments $d_1^u \approx d_1^d \approx d_1^{u+d}/2$, an assumption that is justified in the large-N_c limit (Goeke, Polyakov, and Vanderhaeghen, 2001). Under these approximations, it follows from Eq. (31) that

$$\mathcal{C}_{\mathcal{H}}(t) \approx \tfrac{10}{9} d_1^{u+d}(t) = \tfrac{25}{18} D_{u+d}(t). \quad (40)$$

The truncation in Eq. (30) leads to a systematic uncertainty of *a priori* unknown magnitude. For $Q^2 \to \infty$, the higher-order terms $d_3^q, d_5^q, \ldots$ vanish. But at the Q^2 value that can be reached in the current experiments, they are not necessarily negligible. The results of the chiral quark-soliton model,

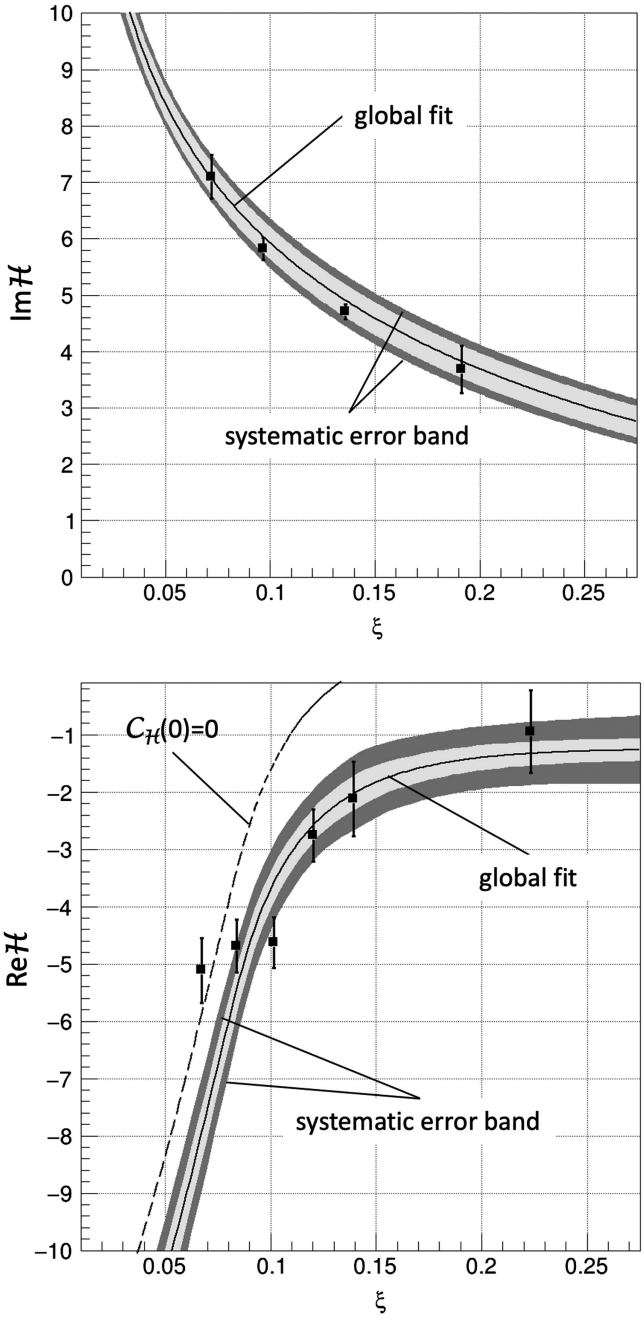

FIG. 10. Top panel: Im$\mathcal{H}$ data points plotted as a function of ξ from local fits to the A_{LU} data (Girod *et al.*, 2008) for $-t = 0.13$–0.15 GeV^2. The central solid line is the global fit constrained by the data points. The light gray error band is due to the uncertainty of the other CFFs. The outer dark gray band shows the total systematic uncertainty to the imaginary part of the fit. Bottom panel: Re$\mathcal{H}$ data extracted from unpolarized cross-section data (Jo *et al.*, 2015). The central solid curve shows the result of the global fit with the dispersion relation applied and the fit parameters of the multipolar form for $\mathcal{C}_{\mathcal{H}}(t)$. The other lines and bands describe the same contribution as for Im$\mathcal{H}$ propagated with the dispersion relation. The dashed line separated from the error bands shows the real part of the amplitude computed from the imaginary part using the dispersion relation and setting $\mathcal{C}_{\mathcal{H}}(0)$ to zero. The difference between the dashed line and the solid line shows the effect of the subtraction term. Note that all markers in Re$\mathcal{H}$ contribute to the precision of a single $-t$ value in $\mathcal{C}_{\mathcal{H}}(t)$, resulting in a small fit uncertainty.

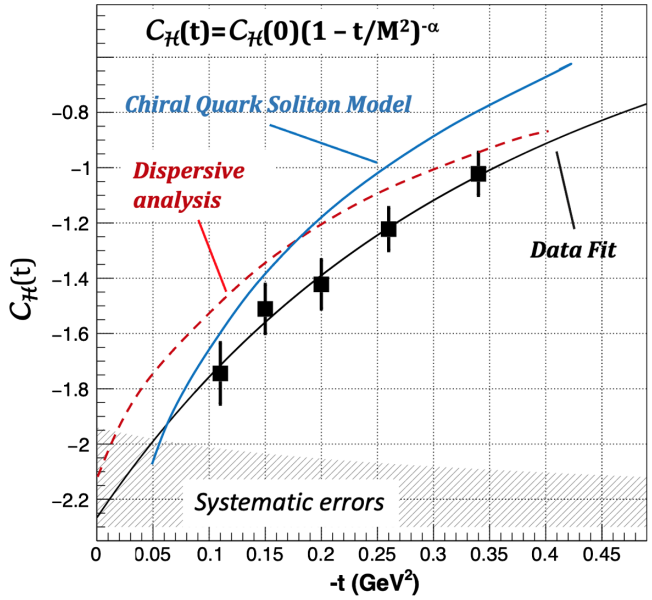

FIG. 11. Subtraction term $\mathcal{C}_{\mathcal{H}}(t)$ as determined from the dispersion relation in the global fit (markers). The uncertainties represent results of the fit errors. The hatched area at the bottom represents the estimated systematic uncertainties described in Fig. 10 for one of the bins in $-t$. The dashed and solid blue curves show the dispersive calculation (Pasquini, Polyakov, and Vanderhaeghen, 2014) and the chiral quark-soliton model predictions (Goeke, Grabis, Ossmann, Polyakov *et al.*, 2007), respectively. Adapted from Burkert, Elouadrhiri, and Girod, 2018.

which predicts values of d_1^{u+d} close to findings in the experimental analysis (Goeke, Grabis, Ossmann, Polyakov *et al.*, 2007), can been used to estimate the contribution of the d_3^q term. At the kinematics relevant for this analysis a ratio $d_3^{u+d}/d_1^{u+d} \approx 0.3$ was found (Kivel, Polyakov, and Vanderhaeghen, 2001). A systematic uncertainty of $\delta(d_1^{u+d})/d_1^{u+d} = \pm 0.30$ has therefore been included in the results of Burkert, Elouadrhiri, and Girod (2018) for $d_1^{u+d}(t)$.

One may ask whether the first two terms in the Gegenbauer polynomial expansion $d_1^q(t)$ and $d_3^q(t)$ could be separated in some way to reduce the systematics. This was studied by Dutrieux *et al.* (2021) by including the Q^2 evolution in the phenomenological analysis. It was found that, assuming the same t dependence, the two terms cannot currently be separated given the limited range in Q^2 covered by the data. In the future one could expect lattice QCD to be able to provide a model-independent evaluation of this higher-order contribution.

We conclude this section by remarking that the determination of $\mathcal{C}_{\mathcal{H}}(t)$ suggests that the quark contribution $\sum_q D_q(t)$ to the proton's GFF $D(t)$ is nonzero and large. These results were supported in a recent paper on the first measurement of TCS (Chatagnon *et al.*, 2021), as shown in Fig. 12, where the contribution of the D-term to the forward-backward asymmetry is seen to be significant. Moreover, the predictions in the chiral quark-soliton model (Goeke, Grabis, Ossmann, Polyakov *et al.*, 2007) and from dispersive analysis (Pasquini, Polyakov, and Vanderhaeghen, 2014) shown in Fig. 11 are consistent with the results discussed here within the systematic uncertainties.

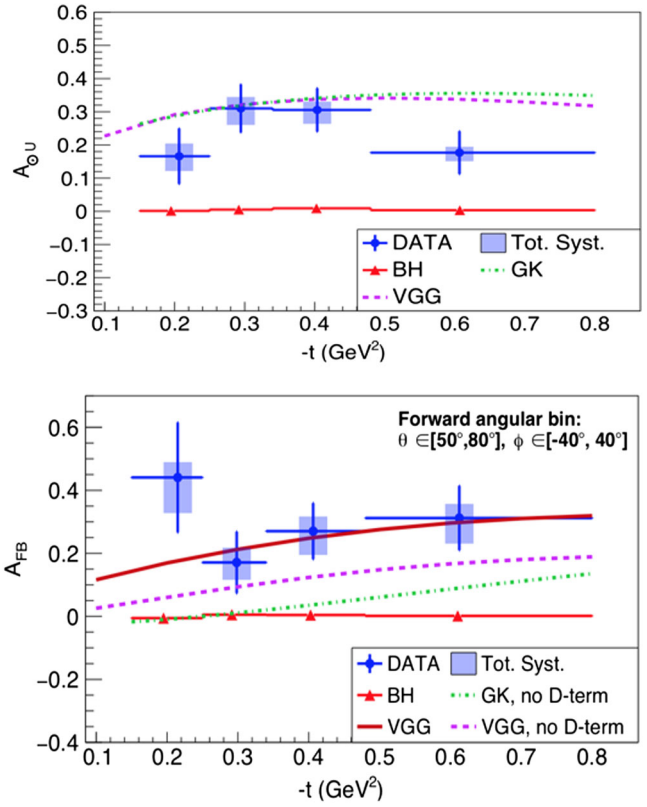

FIG. 12. TCS polarized BSA (top panel) and TCS A_{FB} (bottom panel) for an average 1.8 GeV mass of the timelike photon $M_{e^+e^-}$. A value for A_{LU} of 20%–25% is consistent with what is measured in DVCS and projects out to Im$\mathcal{H}$. The FBA projects out to Re$\mathcal{H}$, which relates directly to the proton's $D_q(t)$ term. The data require the presence of the D-term, as is evident from the difference between the dashed magenta line and the solid red line. At the kinematics of the data in Fig. 11, about half of the asymmetry may be due to the D-term when calculations without and with the D-term are compared (Vanderhaeghen, Guichon, and Guidal, 1999; Pasquini, Polyakov, and Vanderhaeghen, 2014). Adapted from Chatagnon *et al.*, 2021.

C. Other measurements and phenomenological studies

The first extraction of the π^0 GFFs in the timelike region based on the process $\gamma\gamma^* \to \pi^0\pi^0$ (depicted in Fig. 3), which was measured in the Belle experiment in e^+e^- collisions (Masuda *et al.*, 2016), was obtained by Kumano, Song, and Teryaev (2018). For the quark contribution to the π^0 D-term, the value $\sum_q D_q(0) \approx -0.75$ was reported, but systematic uncertainties have not been estimated. It was recently observed by Lorcé, Pire, and Song (2022) that kinematical corrections may significantly impact the extraction of generalized distribution amplitudes from experimental data and should be taken into account in future analyses.

Based on data from experiments at JLab on the energy dependence of J/Ψ production at threshold (Ali *et al.*, 2019; Duran *et al.*, 2023), phenomenological information on the gluon $D_G(t)$ form factor of the proton was extracted (Kharzeev, 2021; Kou, Wang, and Chen, 2021; Wang, Zeng, and Wang, 2022), and estimates were obtained for the gluon contributions to the proton mean square mass radius $\int d^3r\, r^2 \mathcal{T}^{00}(\vec{r})/M_N$ and the mean square scalar radius $\int d^3r\, r^2 g_{\mu\nu}\mathcal{T}^{\mu\nu}(\vec{r})/M_N$. The most recent data on this process were reported by Adhikari *et al.* (2023). (For remarks on the theoretical status of this process, see Sec. III.E.) A similar study for the lighter ϕ meson was presented by Hatta and Strikman (2021).

D. Future experimental developments to access GFFs

As discussed in Sec. III, measurements of DVCS have thus far been most effective in obtaining information related to GPDs. However, there are different experimental processes that can be employed to provide additional, or independent, information on the GPDs and GFFs.

Implementation of a high-duty-cycle positron source, both polarized and unpolarized (Abbott *et al.*, 2016), at JLab would significantly enhance its capabilities in the extraction of the CFF Re$\mathcal{H}(\xi, t)$, and thus of the gravitational form factor $D_q(t)$ and the mechanical properties of the proton.

The timelike Compton scattering process will be measured in parallel to DVCS processes employing large acceptance detector systems such as CLAS12 (Burkert *et al.*, 2020). The TCS event rate is much reduced compared to DVCS and requires higher luminosity for a similar sensitivity to $\mathcal{H}$. In experiments employing large acceptance detector systems, both DVCS and TCS processes are measured simultaneously, in quasireal photoproduction at small $Q^2 \to 0$, and in real photoproduction, where the external production target acts as a radiator of real photons that undergo TCS further downstream in the same target cell.

The double DVCS process enables access to GPDs in their full kinematic dependencies on x, ξ, and t; see Sec. III. At the same time it is reduced in rate by orders of magnitude compared to DVCS (Kopeliovich, Schmidt, and Siddikov, 2010), requiring higher luminosity than is currently achievable. Nevertheless, special equipment that would comply with such requirements has been proposed (Chen *et al.*, 2014). Such measurements are currently planned at JLab in Hall A and Hall B.

Finally, an energy doubling of the existing electron accelerator at JLab is currently under consideration (Arrington *et al.*, 2022). This upgrade would extend the DVCS program to higher Q^2 and lower x_B and better link the DVCS measurements at the current 12 GeV operation to the kinematic reach that will be available at the Electron-Ion Collider, a flagship future facility in preparation at the Brookhaven National Laboratory (discussed later). It will also more fully open the charm sector to access the gluon GFFs.

VI. INTERPRETATION

In Sec. II various properties of the GFFs were discussed at zero momentum transfer. Much of the recent interest in GFFs comes from the fact that they contain information on the spatial distributions of energy, angular momentum, and internal forces that can be accessed at nonzero momentum transfer t via an interpretation that is reviewed here.

A. Static EMT

The 3D interpretation (Polyakov, 2003) of the information encoded by GFFs in Eq. (10) provides analogies to intuitive concepts such as pressure. A 2D interpretation can also be carried out in other frames (Lorcé, Moutarde, and Trawiński, 2019; Freese and Miller, 2021, 2022), with Abel transformations allowing one to relate 2D and 3D interpretations (Panteleeva and Polyakov, 2021).

Considering 2D EMT distributions for a nucleon state boosted to the infinite-momentum frame has the advantage that in this case the nucleon can be perfectly localized around the transverse center of momentum (Burkardt, 2000). In other frames or in three dimensions, an exact probabilistic parton density interpretation does not hold in general. The reservations are analogous to those in the case of, for instance, the interpretation of the electric FF in terms of a 3D electrostatic charge distribution (and a definition of electric mean square charge radius that, despite all caveats, remains a popular concept, giving an idea of the proton's size). The 3D EMT description is nevertheless mathematically rigorous (Polyakov and Schweitzer, 2018b) and can be interpreted in terms of quasiprobabilistic distributions from a phase-space point of view (Lorcé, Moutarde, and Trawiński, 2019; Lorcé, 2020). A strict probabilistic interpretation, however, is justified for heavy nuclei and for the nucleon in the large-N_c limit, where recoil effects can be safely neglected (Polyakov, 2003; Goeke, Grabis, Ossmann, Polyakov *et al.*, 2007; Polyakov and Schweitzer, 2018b; Lorcé, Schweitzer, and Tezgin, 2022).

The meaning of the different components of the static EMT is intuitively clear, with $\mathcal{T}^{00}(\vec{r})$ denoting the energy distribution and $\mathcal{T}^{0k}(\vec{r})$ representing the spatial distribution of momentum. In Secs. VI.B–VI.F the focus is on $\mathcal{T}^{ij}(\vec{r})$, which are perhaps the most interesting components of the static EMT thanks to their relation to the stress tensor and the D-term.

B. The stress tensor and the D-term

The key to the mechanical properties of the proton is the symmetric stress tensor $\mathcal{T}^{ij}(\vec{r})$ given by (Polyakov, 2003)

$$\mathcal{T}^{ij}(\vec{r}) = \left(\frac{r^i r^j}{r^2} - \frac{1}{3}\delta^{ij}\right) s(r) + \delta^{ij} p(r), \tag{41}$$

with $s(r)$ the shear force (or anisotropic stress) and $p(r)$ the pressure with $r = |\vec{r}|$. Both are connected by the differential equation $(2/3)(\mathrm{d}/\mathrm{d}r)s(r) + (2/r)s(r) + (\mathrm{d}/\mathrm{d}r)p(r) = 0$, and $p(r)$ obeys $\int_0^\infty \mathrm{d}r r^2 p(r) = 0$ (Laue, 1911), a necessary but not sufficient condition for stability. These relations originate from the EMT conservation expressed by $\nabla^i \mathcal{T}^{ij}(\vec{r}) = 0$ for the static EMT. The total D-term $D(0)$ can be expressed in terms of $p(r)$ and $s(r)$ in two equivalent ways,

$$D(0) = -\frac{4}{15} M_N \int \mathrm{d}^3 r r^2 s(r) = M_N \int \mathrm{d}^3 r r^2 p(r). \tag{42}$$

The form of the stress tensor (41) is valid for spin-0 and spin-1/2 hadrons; for higher spins see Cosyn *et al.* (2019), Polyakov and Sun (2019), Cotogno *et al.* (2020), Ji and Liu (2021), and Kim and Sun (2021).

If the GFF $D(t)$ is known, then $s(r)$ and $p(r)$ are obtained as follows (Polyakov and Schweitzer, 2018b):

$$s(r) = -\frac{1}{4M_N} r \frac{\mathrm{d}}{\mathrm{d}r} \frac{1}{r} \frac{\mathrm{d}}{\mathrm{d}r} \tilde{D}(r), \tag{43}$$

$$p(r) = \frac{1}{6M_N} \frac{1}{r^2} \frac{\mathrm{d}}{\mathrm{d}r} r^2 \frac{\mathrm{d}}{\mathrm{d}r} \tilde{D}(r), \tag{44}$$

where $\tilde{D}(r) = \int [\mathrm{d}^3\Delta/(2\pi)^3] e^{-i\vec{\Delta}\cdot\vec{r}} D(-\vec{\Delta}^2)$. If the separate $D_q(t)$ and $D_G(t)$ GFFs are known, "partial" quark and gluon shear forces $s_q(r)$ and $s_G(r)$ can be defined in analogy to Eq. (43). To define partial quark and gluon pressures in addition to $D_q(t)$ and $D_G(t)$, knowledge of $\bar{C}_q(t) = -\bar{C}_G(t)$ is required. The latter are responsible for "reshuffling" forces between the gluon and quark subsystems inside the proton (Lorcé, 2018a; Polyakov and Son, 2018) and are difficult to access experimentally. $\bar{C}_q(t)$ was studied in the bag model (Ji, Melnitchouk, and Song, 1997), the chiral quark-soliton model (Goeke, Grabis, Ossmann, Polyakov *et al.*, 2007), the instanton vacuum model (Polyakov and Son, 2018), and lattice QCD (Liu, 2021). Estimates guided by renormalization group methods (Hatta, Rajan, and Tanaka, 2018; Tanaka, 2019; Ahmed, Chen, and Czakon, 2023) yield $\bar{C}_q(0) = -0.163(3)$ at $\mu = 2$ GeV in the $\overline{\mathrm{MS}}$ scheme (Tanaka, 2023).

C. Normal forces and the sign of the D-term

The stress tensor $\mathcal{T}^{ij}(\vec{r})$ can be diagonalized, with one eigenvalue given by the normal force per unit area $p_n(r) = (2/3)s(r) + p(r)$ with the pertinent eigenvector $\vec{e}_r$. The other two eigenvalues are degenerate (for spin 0 and spin 1/2) and are known as tangential forces per unit area $p_t(r) = -(1/3)s(r) + p(r)$, with eigenvectors that can be chosen as unit vectors in the ϑ and φ directions in spherical coordinates (Polyakov and Schweitzer, 2018b).

The normal force appears when considering the force $F^i = \mathcal{T}^{ij}\mathrm{d}S^j = p_n(r)\mathrm{d}S e_r^i$ acting on a radial area element $\mathrm{d}S^j = \mathrm{d}S e_r^j$, where $e_r^j = r^j/r$. General mechanical stability arguments require this force to be directed toward the outside; otherwise, the system will implode. This implies that the normal force per unit area must be positive,

$$p_n(r) = \tfrac{2}{3}s(r) + p(r) > 0. \tag{45}$$

As an immediate consequence of Eq. (45), one concludes by means of Eq. (42) that (Perevalova, Polyakov, and Schweitzer, 2016)

$$D(0) < 0. \tag{46}$$

For hadronic systems like protons, hyperons, mesons, or nuclei for which the D-term has been computed (in models, using chiral perturbation theory, lattice QCD, or dispersive techniques; see Sec. IV) or inferred from experiments (in the cases of the proton and π^0, see Sec. V), it has always been found to be negative, in agreement with Eq. (46).

The aforementioned definitions and conclusions are more than just a fruitful analogy to mechanical systems. At this point it is instructive to recall how one calculates the radii of neutron stars, which are amenable to an unambiguous 3D interpretation. In these macroscopic hadronic systems, general relativity effects cannot be neglected and are incorporated into the Tolman-Oppenheimer-Volkoff equation, which is solved by adopting a model for the nuclear matter equation of state. The solution yields (in our notation) $p_n(r)$ inside the neutron star as a function of the distance r from the center. The obtained solution is positive in the center and decreases monotonically until it drops to zero at some $r = R_*$ and would be negative for $r > R_*$ corresponding to a mechanical instability. This is avoided and a stable solution is obtained by defining $r = R_*$ to be the radius of the neutron star; see Prakash *et al.* (2001). Thus, the point where the normal force per unit area drops to zero coincides with the "edge" of the system.

The proton has no sharp edge, as it is surrounded by a "pion cloud," due to which the normal force does not literally drop to zero but exhibits a Yukawa-type suppression at large r proportional to $(f(r, m_\pi)/r^6)e^{-2m_\pi r}$, where $f(r, m_\pi) \to 1$ when $m_\pi \to 0$ (Goeke, Grabis, Ossmann, Polyakov *et al.*, 2007). In the less realistic but instructive bag model, there is an edge at the bag boundary, where $p_n(r)$ drops to zero (Neubelt *et al.*, 2020). In contrast to the neutron star, one does not determine the edge of the bag model in this way. Instead, the normal force drops automatically to zero at the bag radius, which reflects the fact that from the beginning the bag model was constructed as a simple but mechanically stable model of hadrons (Chodos *et al.*, 1974).

D. The mechanical radius of the proton and neutron

The "size" of the proton is commonly defined through the electric charge distribution, which is indeed a useful concept, though only for charged hadrons. For an electrically neutral hadron like the neutron, the particle size cannot be inferred in this way. In that case, one can still define an electric mean square charge radius $r_{\rm ch}^2 = 6G_E'(0)$ in terms of the derivative of the electric FF $G_E(t)$ at $t = 0$. But for the neutron $r_{\rm ch}^2 < 0$, which provides insight on the distribution of electric charge inside neutron, but not on its size. This is ultimately due to the neutron's charge distribution not being positive definite.

The positive-definite normal force per unit area [Eq. (45)] is an ideal quantity to define the size of the nucleon. One can define the *mechanical radius* as (Polyakov and Schweitzer, 2018a, 2018b)

$$r_{\rm mech}^2 = \frac{\int d^3r\, r^2 p_n(r)}{\int d^3r\, p_n(r)} = \frac{6D(0)}{\int_{-\infty}^{0} dt\, D(t)}. \tag{47}$$

Note that this is an "antiderivative" of a GFF as compared to the electric mean square charge radius defined in terms of the derivative of the electric FF at $t = 0$. With this definition, the proton and neutron have the same radius (modulo isospin violating effects). Note also that the isovector electric mean square charge radius diverges in the chiral limit and is therefore inadequate for defining the proton size in that case, while the mechanical radius in Eq. (47) remains finite in the chiral limit (Polyakov and Schweitzer, 2018b). The mechanical radius of the proton is predicted to be somewhat smaller than its charge radius in soliton models (Cebulla *et al.*, 2007; Goeke, Grabis, Ossmann, Polyakov *et al.*, 2007). The charge and mechanical radii become equal in the nonrelativistic limit that was derived in the bag model (Neubelt *et al.*, 2020; Lorcé, Schweitzer, and Tezgin, 2022).

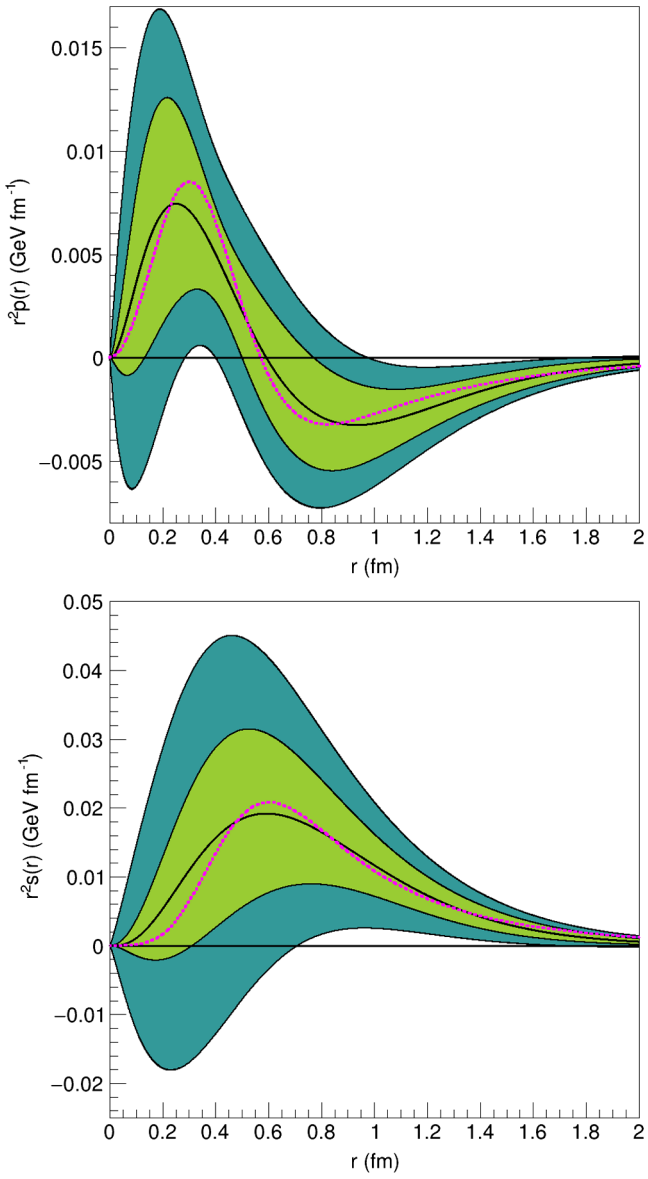

FIG. 13. Distributions of pressure $r^2 p_q(r)$ (top panel) and shear stress $r^2 s_q(r)$ (bottom panel) on quarks in the proton based on JLab data (Burkert, Elouadrhiri, and Girod, 2018, 2021). The central solid lines show the best fits. The outer shaded areas mark the uncertainties when only data prior to the CLAS data are included. The inner shaded areas represent the uncertainties when the CLAS data are used. The widths of the bands are dominated by systematic uncertainties [which include extrapolation into the unmeasured ξ region when one evaluates Eq. (28) and the neglect of higher-order terms in the Gegenbauer expansion described in Eq. (40)]. The dotted magenta curves represent the model predictions of Goeke, Grabis, Ossmann, Polyakov *et al.* (2007).

E. First visualization of forces from experiment

The first visualization of the force distributions in the proton, which was presented by Burkert, Elouadrhiri, and Girod (2018), is reviewed here. As detailed in Sec. V.B, the DVCS data from JLab experiments (Girod *et al.*, 2008; Jo *et al.*, 2015) provided information on the observable $\mathcal{C}_{\mathcal{H}}(t)$ in Eq. (28), from which, under certain reasonable (at present necessary) assumptions, information about the quark contribution $D_{u+d}(t)$ of the proton was deduced. Based on this information, we find that Eq. (44) yields the results for the pressure $p_q(r)$ and the shear force $s_q(r)$ of quarks displayed in Fig. 13 (the index q denotes here $u+d$ quark contributions, with heavier quarks neglected). To obtain $p_q(r)$, Burkert, Elouadrhiri, and Girod (2018) made the additional assumption that $\bar{C}_q(t)$ can be neglected.

The $r^2 p_q(r)$ distribution is positive, peaks near 0.25 fm, changes sign near 0.6 fm, and reaches its minimum value around 1.0 fm. The peak value of $r^2 s_q(r)$ is around 20 MeV fm^{-1}, and occurs near 0.6 fm from the proton's center, where the shear force, given by $4\pi r^2 s_q(r)$, reaches 240 MeV fm^{-1} or 38 kN, an appreciably strong force inside the small proton. Note that these results are consistent with predictions from the chiral quark-soliton model (Goeke, Grabis, Ossmann, Polyakov *et al.*, 2007) within the large systematic uncertainties in the data.

The quark contribution to the normal and tangential forces $p_{n,q}$ and $p_{t,q}(r)$, as defined in Sec. VI.C, are displayed in a two-dimensional plot in Fig. 14. The figure shows the 3D distributions inside the proton in a slice going through the "equatorial plane." The normal forces are strongest at mid distances near 0.5 fm from the proton center and drop toward the center and toward the outer periphery. The tangential forces exhibit a node near 0.40 fm from the center.

F. The *D*-term and long-range forces

Among the open questions in theory is how to define the D-term in the presence of long-range forces. It was shown in a classical model of the proton (Białynicki-Birula, 1993) that $D(t)$ diverges like $1/\sqrt{-t}$ for $t \to 0$ due to the $1/r$ behavior of the Coulomb potential (Varma and Schweitzer, 2020). This result is model independent and was also found for charged pions in chiral perturbation theory (Kubis and Meissner, 2000), in calculations of quantum corrections to the Reissner-Nordström and Kerr-Newman metrics (Donoghue *et al.*, 2002), and for the electron in QED (Metz, Pasquini, and Rodini, 2021).

The deeper reason why $D(t)$ diverges for $t \to 0$ due to QED effects might ultimately be related to the presence of a massless physical state (the photon), which has profound consequences in a theory. Note that $D(t)$ is the only GFF that exhibits this feature when QED effects are included. There are two reasons for this. First, the other proton GFFs are constrained at $t = 0$ [see Eqs. (5) and (6)], while $D(t)$ is not. Second, $D(t)$ is the GFF most sensitive to forces in a system (Hudson and Schweitzer, 2017). Note that $D(t)$ is multiplied by the prefactor $(\Delta^\mu \Delta^\nu - g^{\mu\nu}\Delta^2)$ such that, despite the divergence of $D(t)$ due to QED effects, the matrix element $\langle p'|T_a^{\mu\nu}|p\rangle$ is well behaved in the forward limit.

There have been studies of the D-term for the H atom (Ji and Liu, 2021, 2022), which defy the interpretation presented here. This is perhaps not a surprise, considering the differences between hadronic and atomic bound states.

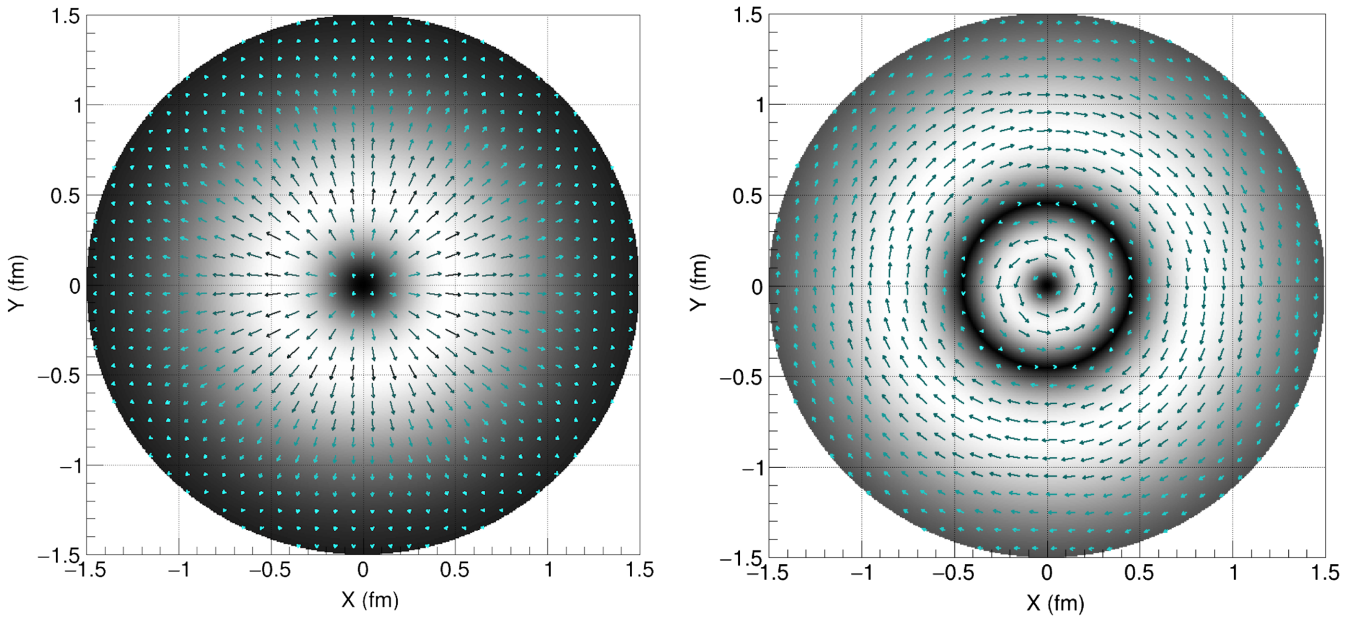

FIG. 14. 2D display of the quark contribution to the distribution of forces in the proton as a function of the distance from the proton's center (Burkert, Elouadrhiri, and Girod, 2021). The light gray shading and longer arrows indicate areas of stronger forces, while the dark shading and shorter arrows indicate areas of weaker forces. Left panel: normal forces as a function of distance from the center. The arrows change magnitude and always point radially outward. Right panel: tangential forces as a function of distance from the center. The force changes direction and magnitude as indicated by the direction and length of the arrow. The forces change sign near 0.4 fm from the proton center.

Atoms are comparatively large, low-density objects. Pressure concepts from continuum mechanics might not apply to atoms whose stability is well understood within nonrelativistic quantum mechanics. In contrast, the proton as a QCD bound state has nearly the same mass as an H atom but a much smaller size ($\sim 10^{-15}$ m) and constitutes a compact high-density system (15 orders of magnitude more dense than an atom) where continuum mechanics concepts can be applied and provide insightful interpretations. Another important aspect might be played by the role of confinement absent for atoms that can be easily ionized. Hadrons constitute a much different type of bound state in this respect. More theoretical work is needed to clarify these issues.

VII. SUMMARY AND OUTLOOK

This Colloquium gives an overview of interesting recent developments along a new avenue of experimental and theoretical studies of the gravitational structure of hadrons, especially the proton. The gravitational form factors of the proton rose to prominence after Ji (1995a, 1997b) illustrated how they can be used to gain insight into fundamental questions such as the following: How much do the gravitational form factors contribute to the mass and the spin of the proton? Soon afterward, Polyakov (2003) showed that quarks and gluons also provide information about the spatial distribution of mass and spin and allow one to study the forces at play in the bound system. These works triggered many follow-up studies and investigations that have deepened our understanding of proton structure.

Through matrix elements of the energy-momentum operator, the gravitational form factors of the proton and other hadrons have been studied in theoretical approaches including a wide range of models and in numerical calculations in the framework of lattice QCD. In broad terms, the simplest aspects of the EMT structure of the proton and other hadrons (such as the pion) have been understood from theory for many years, and first-principles calculations providing complete and controlled decompositions of the proton's mass and spin, for example, are now available. Conversely, more complicated aspects of proton and nuclear structure, such as gluon gravitational form factors, the x dependence of generalized parton distributions, and energy-momentum tensor matrix elements in light nuclei, were computed for the first time in the last several years, as yet without complete systematic control, and significant progress can be expected over the next decade. Theoretical insight into these fundamental aspects of proton and nuclear structure is thus currently in a phase of rapid progress, complementing the improvement of experimental constraints on these quantities and providing predictions for future experiments.

The first experimental results discussed in this Colloquium are based on precise measurements of the deeply virtual Compton scattering process with a polarized electron beam that determines both the beam-spin asymmetry and the absolute differential cross section of $\vec{e}p \to ep\gamma$. Measurements covered a limited range in the kinematic variables, which made it necessary to employ information from high-energy collider data to constrain the global data fit in the region that was not covered in the CLAS experiment. Consequently, large systematic uncertainties were assigned to the results.

New experimental results on DVCS measurements with polarized electron beams at higher energy have recently been published from experiments with CLAS12 (Christiaens *et al.*, 2022) and from Hall A at Jefferson Laboratory (Georges *et al.*, 2022). These measurements extend the kinematic reach both to higher and to lower values in ξ and increase the range covered in Q^2. The latter will allow for more sensitive measurements of the Q^2 evolution of the DVCS cross section. These new data may also support the application of machine learning techniques and artificial neural networks in the higher level data analysis as have been developed by several groups (Berthou *et al.*, 2018; Kumerički, 2019; Grigsby *et al.*, 2021).

Ongoing experiments and future planned measurements that employ proton and deuterium (neutron) targets, spin polarized transversely to the beam direction, have strong sensitivity to CFF $\mathcal{E}$. Precise knowledge of the kinematic dependence of $\mathcal{E}(\xi, t)$ is needed to measure the quark angular momentum distribution encoded in the GFF $J_q(t)$ of the proton (Ji, 1997b), as defined in Sec. II.A.

The plan to extend Jefferson Lab's electron accelerator energy reach to 22 GeV would more fully open access to employing J/Ψ production near threshold in a wide t range, and in some ξ range to access the gluon part $D_G(t)$ of the proton's D-term.

DVCS data from the COMPASS experiment at CERN with 160 GeV of oppositely polarized μ^+ and μ^- beams (Akhunzyanov *et al.*, 2019) reach smaller ξ values and into the sea-quark region. The average of the measured μ^+ and μ^- cross sections allows for the determination of $\mathrm{Im}\mathcal{H}$. Results from high statistics runs that cover the lower x_B domain are expected in the near future. With these new data, the difference of μ^+ and μ^- cross sections can also be formed to obtain the charge asymmetry, which provides direct access to $\mathrm{Re}\mathcal{H}$.

A long-term perspective is provided by the planned Electron-Ion Collider projects in the U.S. (Abdul Khalek *et al.*, 2022; Burkert *et al.*, 2023) and China (Anderle *et al.*, 2021). The U.S. project will extend the kinematic reach in $x_B > 10^{-4}$ and thus cover the gluon dominated domain with high operational luminosity up to 10^{34} cm^{-2} s^{-1}. It features polarized electron and polarized proton beams, the latter longitudinally or transversely polarized, and light ion beams. The Electron-Ion Collider in China focuses on the lower energy domain with $x_B > 10^{-3}$, which connects more closely to the kinematics of the fixed-target experiments at JLab that operate at high luminosity in the valence quark and the $q\bar{q}$-sea domain.

Currently available data allowed for a pioneering first step into this emerging new field of the proton internal structure, complementing what has been learned in many detailed experiments over the past 70 years of studies of the proton electromagnetic structure, with the first result given on the proton's mechanical structure. This new avenue of research has been rapidly developing theoretically, and the first experimental results on the proton firmly established the study of mechanical properties of subatomic particles as an interesting new field of fundamental science. Many objects on Earth, in the Solar System, and in the Universe are described

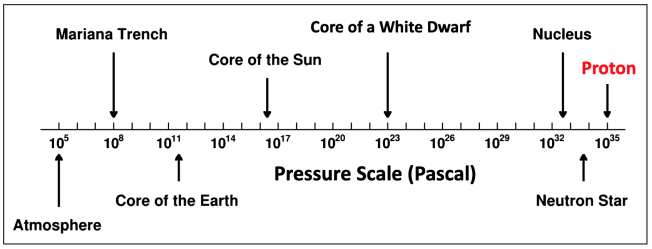

FIG. 15. Comparison of peak pressures inside various objects on Earth, in the Solar System, and in the Universe.

by their equation of state, where the internal pressure plays an essential role. Some of these objects are included in Fig. 15. The study discussed in this Colloquium adds the smallest object with the highest internal pressure to this list of objects that have been studied thus far. The peak pressure inside the proton is approximately 10^{35} Pa. It tops by 30 orders of magnitude the atmospheric pressure on Earth. It even exceeds the pressure in the core of the most densely packed known macroscopic objects in the Universe, neutron stars, which was given as 1.6×10^{34} Pa by Özel and Freire (2016). Other subatomic objects such as pions, kaons, hyperons, and light and heavy nuclei may be the subjects of experimental investigation in the future. The scientific instruments needed to study them efficiently are in preparation.

The gravitational form factors provide the key to address fundamental questions about the mass, spin, and internal forces inside the proton and other hadrons. Theoretical, experimental, and phenomenological studies of gravitational form factors provide interesting insights. In this emerging field, there are many lessons to learn and there is much to look forward to.

LIST OF SYMBOLS AND ABBREVIATIONS

AM	angular momentum
BSA	beam-spin asymmetry
CFF	Compton form factor
DIS	deep inelastic scattering
DVCS	deeply virtual Compton scattering
EMT	energy-momentum tensor
FF	form factor
GFF	gravitational form factor
GPD	generalized parton distribution
JLab	Jefferson Lab
PDF	parton distribution function
QCD	quantum chromodynamics
QED	quantum electrodynamics
TCS	timelike Compton scattering

ACKNOWLEDGMENTS

We cannot mention the names of all colleagues or acknowledge all discussions during or prior to the preparation of this Colloquium. We name only Maxim Polyakov, who until his untimely death in August 2021 influenced or initiated many of the reviewed topics. Special thanks go to Joanna Griffin for professional assistance with preparing the diagrams and figures. This material is based upon work supported by the U.S. Department of Energy, Office of Science, Office of Nuclear Physics, under Contract No. DE-AC05-06OR23177. P. S. was supported by a NSF grant under Contract No. 2111490. P. E. S. was supported in part by the U.S. Department of Energy, Office of Science, Office of Nuclear Physics, under Grant Contract No. DE-SC0011090 and by Early Career Award No. DE-SC0021006, by an NEC research award, and by the Carl G. and Shirley Sontheimer Research Fund. This work was supported in part by the Department of Energy within the framework of the QGT Topical Collaboration.

REFERENCES

Abbott, D., *et al.* (PEPPo Collaboration), 2016, "Production of Highly Polarized Positrons Using Polarized Electrons at MeV Energies," Phys. Rev. Lett. **116**, 214801.

Abdul Khalek, R., *et al.*, 2022, "Science requirements and detector concepts for the Electron-Ion Collider: EIC yellow report," Nucl. Phys. **A1026**, 122447.

Abidin, Zainul, and Carl E. Carlson, 2008, "Gravitational form factors in the axial sector from an AdS/QCD model," Phys. Rev. D **77**, 115021.

Abidin, Zainul, and Carl E. Carlson, 2009, "Nucleon electromagnetic and gravitational form factors from holography," Phys. Rev. D **79**, 115003.

Adhikari, S., *et al.* (GlueX Collaboration), 2023, "Measurement of the J/ψ photoproduction cross section over the full near-threshold kinematic region," arXiv:2304.03845.

Adloff, C., *et al.* (H1 Collaboration), 2001, "Measurement of deeply virtual Compton scattering at HERA," Phys. Lett. B **517**, 47–58.

Ahmed, Taushif, Long Chen, and Michał Czakon, 2023, "A note on quark and gluon energy-momentum tensors," J. High Energy Phys. 01, 077.

Aidala, Christine A., Steven D. Bass, Delia Hasch, and Gerhard K. Mallot, 2013, "The spin structure of the nucleon," Rev. Mod. Phys. **85**, 655–691.

Airapetian, A., *et al.* (HERMES Collaboration), 2001, "Measurement of the Beam Spin Azimuthal Asymmetry Associated with Deeply Virtual Compton Scattering," Phys. Rev. Lett. **87**, 182001.

Akhunzyanov, R., *et al.* (COMPASS Collaboration), 2019, "Transverse extension of partons in the proton probed in the sea-quark range by measuring the DVCS cross section," Phys. Lett. B **793**, 188–194; **800**, 135129(E) (2020).

Alexandrou, C., S. Bacchio, M. Constantinou, J. Finkenrath, K. Hadjiyiannakou, K. Jansen, G. Koutsou, H. Panagopoulos, and G. Spanoudes (Extended Twisted Mass Collaboration), 2020a, "Complete flavor decomposition of the spin and momentum fraction of the proton using lattice QCD simulations at physical pion mass," Phys. Rev. D **101**, 094513.

Alexandrou, C., S. Bacchio, M. Constantinou, J. Finkenrath, K. Hadjiyiannakou, K. Jansen, G. Koutsou, and A. Vaquero Aviles-Casco, 2020b, "Nucleon axial, tensor, and scalar charges and σ-terms in lattice QCD", Phys. Rev. D **102**, 054517.

Alexandrou, C., M. Constantinou, K. Hadjiyiannakou, K. Jansen, C. Kallidonis, G. Koutsou, A. Vaquero Avilés-Casco, and C. Wiese, 2017, "Nucleon Spin and Momentum Decomposition Using Lattice QCD Simulations," Phys. Rev. Lett. **119**, 142002.

Alexandrou, C., *et al.*, 2020, "Moments of nucleon generalized parton distributions from lattice QCD simulations at physical pion mass," Phys. Rev. D **101**, 034519.

Alexandrou, Constantia, Krzysztof Cichy, Martha Constantinou, Kyriakos Hadjiyiannakou, Karl Jansen, Aurora Scapellato, and Fernanda Steffens, 2020, "Unpolarized and Helicity Generalized Parton Distributions of the Proton within Lattice QCD," Phys. Rev. Lett. **125**, 262001.

Alexandrou, Constantia, Martha Constantinou, Kyriakos Hadjiyiannakou, Karl Jansen, Christos Kallidonis, Giannis Koutsou, and Alejandro Vaquero Avilés-Casco, 2018, "Nucleon spin structure from lattice QCD," Proc. Sci. DIS2018, 148 [arXiv:1807.11214].

Alharazin, H., D. Djukanovic, J. Gegelia, and M. V. Polyakov, 2020, "Chiral theory of nucleons and pions in the presence of an external gravitational field," Phys. Rev. D **102**, 076023.

Alharazin, H., E. Epelbaum, J. Gegelia, U. G. Meißner, and B. D. Sun, 2022, "Gravitational form factors of the delta resonance in chiral EFT," Eur. Phys. J. C **82**, 907.

Ali, A., *et al.* (GlueX Collaboration), 2019, "First Measurement of Near-Threshold J/ψ Exclusive Photoproduction off the Proton," Phys. Rev. Lett. **123**, 072001.

Aliev, T. M., K. Şimşek, and T. Barakat, 2021, "Gravitational formfactors of the ρ, π, and K mesons in the light-cone QCD sum rules," Phys. Rev. D **103**, 054001.

Alvarez, Luis W., and F. Bloch, 1940, "A Quantitative determination of the neutron moment in absolute nuclear magnetons," Phys. Rev. **57**, 111–122.

Amor-Quiroz, Arturo, William Focillon, Cédric Lorcé, and Simone Rodini, 2023, "Energy-momentum tensor in the scalar diquark model," arXiv:2304.10339.

Anderle, Daniele P., *et al.*, 2021, "Electron-ion collider in China," Front. Phys. **16**, 64701.

Anikin, I. V., 2019, "Gravitational form factors within light-cone sum rules at leading order," Phys. Rev. D **99**, 094026.

Anikin, I. V., and O. V. Teryaev, 2008, "Dispersion relations and QCD factorization in hard reactions," Fiz. B **17**, 151–158 [arXiv:0710.4211v2].

Arrington, J., *et al.*, 2022, "Physics with CEBAF at 12 GeV and future opportunities," Prog. Part. Nucl. Phys. **127**, 103985.

Azizi, K., and U. Özdem, 2020, "Nucleon's energy-momentum tensor form factors in light-cone QCD," Eur. Phys. J. C **80**, 104.

Azizi, K., and U. Özdem, 2021, "Gravitational form factors of $N(1535)$ in QCD," Nucl. Phys. **A1015**, 122296.

Bakker, B. L. G., E. Leader, and T. L. Trueman, 2004, "Critique of the angular momentum sum rules and a new angular momentum sum rule," Phys. Rev. D **70**, 114001.

Bali, Gunnar, Sara Collins, Meinulf Göckeler, Rudolf Rödl, Andreas Schäfer, and Andre Sternbeck, 2016, "Nucleon generalized form factors from lattice QCD with nearly physical quark masses," Proc. Sci. LATTICE2015, 118 [arXiv:1601.04818].

Belinfante, Frederik J., 1962, "Consequences of the postulate of a complete commuting set of observables in quantum electrodynamics," Phys. Rev. **128**, 2832–2837.

Belitsky, Andrei V., and X. Ji, 2002, "Chiral structure of nucleon gravitational form-factors," Phys. Lett. B **538**, 289–297.

Belitsky, Andrei V., and Dieter Müller, 2003, "Exclusive Electroproduction of Lepton Pairs as a Probe of Nucleon Structure," Phys. Rev. Lett. **90**, 022001.

Belitsky, Andrei V., Dieter Müller, and A. Kirchner, 2002, "Theory of deeply virtual Compton scattering on the nucleon," Nucl. Phys. **B629**, 323–392.

Berger, Edgar R., M. Diehl, and B. Pire, 2002, "Time-like Compton scattering: Exclusive photoproduction of lepton pairs," Eur. Phys. J. C **23**, 675–689.

Berthou, B., *et al.*, 2018, "PARTONS: PARtonic Tomography Of Nucleon Software: A computing framework for the phenomenology of generalized parton distributions," Eur. Phys. J. C **78**, 478.

Bertone, V., H. Dutrieux, C. Mezrag, H. Moutarde, and P. Sznajder, 2021, "Deconvolution problem of deeply virtual Compton scattering," Phys. Rev. D **103**, 114019.

Białynicki-Birula, Iwo, 1993, "Simple relativistic model of a finite size particle," Phys. Lett. A **182**, 346–352.

Bjorken, J. D., 1969, "Asymptotic sum rules at infinite momentum," Phys. Rev. **179**, 1547–1553.

Bloom, Elliott D., *et al.*, 1969, "High-Energy Inelastic e-p Scattering at 6° and 10°," Phys. Rev. Lett. **23**, 930–934.

Boussarie, R., B. Pire, L. Szymanowski, and S. Wallon, 2017, "Exclusive photoproduction of a $\gamma\rho$ pair with a large invariant mass," J. High Energy Phys. 02, 054; 10 (2020) 029(E).

Brandelik, R., *et al.* (TASSO Collaboration), 1980, "Evidence for a spin one gluon in three jet events," Phys. Lett. **97B**, 453–458.

Braun, V. M., G. P. Korchemsky, and Dieter Müller, 2003, "The uses of conformal symmetry in QCD," Prog. Part. Nucl. Phys. **51**, 311–398.

Brodsky, Stanley J., Dae Sung Hwang, Bo-Qiang Ma, and Ivan Schmidt, 2001, "Light cone representation of the spin and orbital angular momentum of relativistic composite systems," Nucl. Phys. **B593**, 311–335.

Brodsky, Stanley J., and Guy F. de Teramond, 2008, "Light-front dynamics and AdS/QCD correspondence: Gravitational form factors of composite hadrons," Phys. Rev. D **78**, 025032.

Brömmel, D., M. Diehl, M. Göckeler, Ph. Hägler, R. Horsley, D. Pleiter, Paul E. L. Rakow, A. Schäfer, G. Schierholz, and J. M. Zanotti, 2006, "Structure of the pion from full lattice QCD," Proc. Sci. LAT2005, 360 [arXiv:hep-lat/0509133].

Brömmel, Dirk, 2007, "Pion structure from the lattice," Ph.D. thesis (University of Regensburg).

Burkardt, Matthias, 2000, "Impact parameter dependent parton distributions and off forward parton distributions for $\zeta \to 0$," Phys. Rev. D **62**, 071503; **66**, 119903(E) (2002).

Burkert, V., *et al.* (CLAS Collaboration), 2021, "Beam charge asymmetries for deeply virtual Compton scattering off the proton," Eur. Phys. J. A **57**, 186.

Burkert, V. D., L. Elouadrhiri, and F. X. Girod, 2018, "The pressure distribution inside the proton," Nature (London) **557**, 396–399.

Burkert, V. D., L. Elouadrhiri, and F. X. Girod, 2021, "Determination of shear forces inside the proton," arXiv:2104.02031.

Burkert, V. D., *et al.*, 2020, "The CLAS12 Spectrometer at Jefferson Laboratory," Nucl. Instrum. Methods Phys. Res., Sect. A **959**, 163419.

Burkert, V. D., *et al.*, 2023, "Precision studies of QCD in the low energy domain of the EIC," Prog. Part. Nucl. Phys. **131**, 104032.

Cantara, Michael, Manuel Mai, and Peter Schweitzer, 2016, "The energy-momentum tensor and D-term of Q-clouds," Nucl. Phys. **A953**, 1–20.

Cebulla, C., K. Goeke, J. Ossmann, and P. Schweitzer, 2007, "The nucleon form-factors of the energy momentum tensor in the Skyrme model," Nucl. Phys. **A794**, 87–114.

Chadwick, J., 1932, "Possible existence of a neutron," Nature (London) **129**, 312.

Chakrabarti, Dipankar, Chandan Mondal, and Asmita Mukherjee, 2015, "Gravitational form factors and transverse spin sum rule in a light front quark-diquark model in AdS/QCD," Phys. Rev. D **91**, 114026.

Chakrabarti, Dipankar, Chandan Mondal, Asmita Mukherjee, Sreeraj Nair, and Xingbo Zhao, 2020, "Gravitational form factors and mechanical properties of proton in a light-front quark-diquark model," Phys. Rev. D **102**, 113011.

Chambers, A. J., R. Horsley, Y. Nakamura, H. Perlt, P. E. L. Rakow, G. Schierholz, A. Schiller, K. Somfleth, R. D. Young, and J. M. Zanotti, 2017, "Nucleon Structure Functions from Operator Product Expansion on the Lattice," Phys. Rev. Lett. **118**, 242001.

Chatagnon, P., *et al.* (CLAS Collaboration), 2021, "First Measurement of Timelike Compton Scattering," Phys. Rev. Lett. **127**, 262501.

Chekanov, S., *et al.* (ZEUS Collaboration), 2003, "Measurement of deeply virtual Compton scattering at HERA," Phys. Lett. B **573**, 46–62.

Chen, J. P., H. Gao, T. K. Hemmick, Z. E. Meziani, and P. A. Souder (SoLID Collaboration), 2014, "A white paper on SoLID (Solenoidal Large Intensity Device)," arXiv:1409.7741.

Chen, Xiang-Song, Xiao-Fu Lu, Wei-Min Sun, Fan Wang, and T. Goldman, 2008, "Spin and Orbital Angular Momentum in Gauge Theories: Nucleon Spin Structure and Multipole Radiation Revisited," Phys. Rev. Lett. **100**, 232002.

Chen, Yi, and Cédric Lorcé, 2022, "Pion and nucleon relativistic electromagnetic four-current distributions," Phys. Rev. D **106**, 116024.

Chen, Yi, and Cédric Lorcé, 2023, "Nucleon relativistic polarization and magnetization distributions," Phys. Rev. D **107**, 096003.

Chodos, A., R. L. Jaffe, K. Johnson, Charles B. Thorn, and V. F. Weisskopf, 1974, "New extended model of hadrons," Phys. Rev. D **9**, 3471–3495.

Choudhary, Poonam, Bheemsehan Gurjar, Dipankar Chakrabarti, and Asmita Mukherjee, 2022, "Gravitational form factors and mechanical properties of the proton: Connections between distributions in 2D and 3D," Phys. Rev. D **106**, 076004.

Christiaens, G., *et al.* (CLAS Collaboration), 2022, "First CLAS12 measurement of DVCS beam-spin asymmetries in the extended valence region," arXiv:2211.11274.

Collins, John C., Anthony Duncan, and Satish D. Joglekar, 1977, "Trace and dilatation anomalies in gauge theories," Phys. Rev. D **16**, 438–449.

Collins, John C., Leonid Frankfurt, and Mark Strikman, 1997, "Factorization for hard exclusive electroproduction of mesons in QCD," Phys. Rev. D **56**, 2982–3006.

Collins, John C., and Andreas Freund, 1999, "Proof of factorization for deeply virtual Compton scattering in QCD," Phys. Rev. D **59**, 074009.

Constantinou, Martha, *et al.*, 2021, "Parton distributions and lattice-QCD calculations: Toward 3D structure," Prog. Part. Nucl. Phys. **121**, 103908.

Cosyn, Wim, Sabrina Cotogno, Adam Freese, and Cédric Lorcé, 2019, "The energy-momentum tensor of spin-1 hadrons: Formalism," Eur. Phys. J. C **79**, 476.

Cotogno, Sabrina, Cédric Lorcé, and Peter Lowdon, 2019, "Poincaré constraints on the gravitational form factors for massive states with arbitrary spin," Phys. Rev. D **100**, 045003.

Cotogno, Sabrina, Cédric Lorcé, Peter Lowdon, and Manuel Morales, 2020, "Covariant multipole expansion of local currents for massive states of any spin," Phys. Rev. D **101**, 056016.

Dashen, Roger F., Elizabeth Ellen Jenkins, and Aneesh V. Manohar, 1994, "The $1/N_c$ expansion for baryons," Phys. Rev. D **49**, 4713; **51**, 2489(E) (1995).

Detmold, W., D. Pefkou, and P. E. Shanahan, 2017, "Off-forward gluonic structure of vector mesons," Phys. Rev. D **95**, 114515.

Detmold, William, and C. J. David Lin, 2006, "Deep-inelastic scattering and the operator product expansion in lattice QCD," Phys. Rev. D **73**, 014501.

Detmold, William, Anthony V. Grebe, Issaku Kanamori, C. J. David Lin, Robert J. Perry, and Yong Zhao (HOPE Collaboration), 2021, "Parton physics from a heavy-quark operator product expansion: Formalism and Wilson coefficients," Phys. Rev. D **104**, 074511.

Detmold, William, Marc Illa, David J. Murphy, Patrick Oare, Kostas Orginos, Phiala E. Shanahan, Michael L. Wagman, and Frank Winter (NPLQCD Collaboration), 2021, "Lattice QCD Constraints on the Parton Distribution Functions of ^{3}He," Phys. Rev. Lett. **126**, 202001.

d'Hose, Nicole, Silvia Niccolai, and Armine Rostomyan, 2016, "Experimental overview of deeply virtual Compton scattering," Eur. Phys. J. A **52**, 151.

Diehl, M., T. Gousset, B. Pire, and O. Teryaev, 1998, "Probing Partonic Structure in $\gamma^*\gamma \to \pi\pi$ near Threshold," Phys. Rev. Lett. **81**, 1782–1785.

Diehl, M., A. Manashov, and A. Schäfer, 2006, "Chiral perturbation theory for nucleon generalized parton distributions," Eur. Phys. J. A **29**, 315–326; **56**, 220(E) (2020).

Diehl, M., and D. Yu. Ivanov, 2007, "Dispersion representations for hard exclusive processes: Beyond the Born approximation," Eur. Phys. J. C **52**, 919–932.

Donoghue, J. F., E. Golowich, and Barry R. Holstein, 2014 *Dynamics of the Standard Model*, Vol. 2 (Cambridge University Press, Cambridge, England).

Donoghue, John F., J. Gasser, and H. Leutwyler, 1990, "The decay of a light Higgs boson," Nucl. Phys. **B343**, 341–368.

Donoghue, John F., Barry R. Holstein, Björn Garbrecht, and Thomas Konstandin, 2002, "Quantum corrections to the Reissner-Nordström and Kerr-Newman metrics," Phys. Lett. B **529**, 132–142; **612**, 311(E)–312(E) (2005).

Donoghue, John F., and H. Leutwyler, 1991, "Energy and momentum in chiral theories," Z. Phys. C **52**, 343–351.

Duplančić, G, K. Passek-Kumerički, B. Pire, L. Szymanowski, and S. Wallon, 2018, "Probing axial quark generalized parton distributions through exclusive photoproduction of a $\gamma\pi^{\pm}$ pair with a large invariant mass," J. High Energy Phys. 11, 179.

Duran, B., *et al.*, 2023, "Determining the gluonic gravitational form factors of the proton," Nature (London) **615**, 813–816.

Dutrieux, H., C. Lorcé, H. Moutarde, P. Sznajder, A. Trawiński, and J. Wagner, 2021, "Phenomenological assessment of proton mechanical properties from deeply virtual Compton scattering," Eur. Phys. J. C **81**, 300.

Engelhardt, M., J. R. Green, N. Hasan, S. Krieg, S. Meinel, J. Negele, A. Pochinsky, and S. Syritsyn, 2020, "From Ji to Jaffe-Manohar orbital angular momentum in lattice QCD using a direct derivative method," Phys. Rev. D **102**, 074505.

Englert, François, 2014, "Nobel Lecture: The BEH mechanism and its scalar boson," Rev. Mod. Phys. **86**, 843.

Epelbaum, E., J. Gegelia, U. G. Meißner, and M. V. Polyakov, 2022, "Chiral theory of ρ-meson gravitational form factors," Phys. Rev. D **105**, 016018.

Feynman, Richard P., 1969, "Very High-Energy Collisions of Hadrons," Phys. Rev. Lett. **23**, 1415–1417.

Fiore, Roberto, Laszlo Jenkovszky, and Maryna Oleksiienko, 2021, "On matter and pressure distribution in nucleons," arXiv:2112.00605.

Freese, Adam, and Wim Cosyn, 2022a, "Spatial densities of momentum and forces in spin-one hadrons," Phys. Rev. D **106**, 114013.

Freese, Adam, and Wim Cosyn, 2022b, "Spatial densities of the photon on the light front," Phys. Rev. D **106**, 114014.
Freese, Adam, and Ian C. Cloët, 2019, "Gravitational form factors of light mesons," Phys. Rev. C **100**, 015201; **105**, 059901(E) (2022).
Freese, Adam, Andreas Metz, Barbara Pasquini, and Simone Rodini, 2023, "The gravitational form factors of the electron in quantum electrodynamics," Phys. Lett. B **839**, 137768.
Freese, Adam, and Gerald A. Miller, 2021, "Forces within hadrons on the light front," Phys. Rev. D **103**, 094023.
Freese, Adam, and Gerald A. Miller, 2022, "Unified formalism for electromagnetic and gravitational probes: Densities," Phys. Rev. D **105**, 014003.
Friot, S., B. Pire, and L. Szymanowski, 2007, "Deeply virtual compton scattering on a photon and generalized parton distributions in the photon," Phys. Lett. B **645**, 153–160.
Frisch, Robert, and Otto Stern, 1933, "Über die magnetische Ablenkung von Wasserstoffmolekülen und das magnetische Moment des Protons. I [The magnetic deflection of hydrogen molecules and the magnetic moment of the proton]," Z. Phys. **85**, 4–16.
Fritzsch, H., Murray Gell-Mann, and H. Leutwyler, 1973, "Advantages of the color octet gluon picture," Phys. Lett. **47B**, 365–368.
Fu, Dongyan, Bao-Dong Sun, and Yubing Dong, 2022, "Electromagnetic and gravitational form factors of Δ resonance in a covariant quark-diquark approach," Phys. Rev. D **105**, 096002.
Fujita, Mitsutoshi, Yoshitaka Hatta, Shigeki Sugimoto, and Takahiro Ueda, 2022, "Nucleon D-term in holographic quantum chromodynamics," Prog. Theor. Exp. Phys. 093B06.
Gabdrakhmanov, I. R., and O. V. Teryaev, 2012, "Analyticity and sum rules for photon GPDs," Phys. Lett. B **716**, 417–424.
García Martín-Caro, Alberto, Miguel Huidobro, and Yoshitaka Hatta, 2023, "Gravitational form factors of nuclei in the Skyrme model," arXiv:2304.05994.
Gegelia, Jambul, and Maxim V. Polyakov, 2021, "A bound on the nucleon Druck-term from chiral EFT in curved space-time and mechanical stability conditions," Phys. Lett. B **820**, 136572.
Gell-Mann, Murray, 1964, "A schematic model of baryons and mesons," Phys. Lett. **8**, 214–215.
Georges, F., *et al.* (Jefferson Lab Hall A Collaboration), 2022, "Deeply Virtual Compton Scattering Cross Section at High Bjorken x_B," Phys. Rev. Lett. **128**, 252002.
Ghim, Nam-Yong, Hyun-Chul Kim, Ulugbek Yakhshiev, and Ghil-Seok Yang, 2023, "Medium modification of singly heavy baryons in a pion-mean-field approach," Phys. Rev. D **107**, 014024.
Girod, F. X., *et al.* (CLAS Collaboration), 2008, "Measurement of Deeply Virtual Compton Scattering Beam-Spin Asymmetries," Phys. Rev. Lett. **100**, 162002.
Goeke, K., J. Grabis, J. Ossmann, M. V. Polyakov, P. Schweitzer, A. Silva, and D. Urbano, 2007, "Nucleon form factors of the energy momentum tensor in the chiral quark-soliton model," Phys. Rev. D **75**, 094021.
Goeke, K., J. Grabis, J. Ossmann, P. Schweitzer, A. Silva, and D. Urbano, 2007, "The pion mass dependence of the nucleon form factors of the energy momentum tensor in the chiral quark-soliton model," Phys. Rev. C **75**, 055207.
Goeke, K., Maxim V. Polyakov, and M. Vanderhaeghen, 2001, "Hard exclusive reactions and the structure of hadrons," Prog. Part. Nucl. Phys. **47**, 401–515.
Grigsby, Jake, Brandon Kriesten, Joshua Hoskins, Simonetta Liuti, Peter Alonzi, and Matthias Burkardt, 2021, "Deep learning analysis of deeply virtual exclusive photoproduction," Phys. Rev. D **104**, 016001.
Grocholski, Oskar, Bernard Pire, Paweł Sznajder, Lech Szymanowski, and Jakub Wagner, 2022, "Phenomenology of diphoton photoproduction at next-to-leading order," Phys. Rev. D **105**, 094025.
Gross, David J., and Frank Wilczek, 1973, "Ultraviolet Behavior of Non-Abelian Gauge Theories," Phys. Rev. Lett. **30**, 1343–1346.
Guidal, M., and M. Vanderhaeghen, 2003, "Double Deeply Virtual Compton Scattering off the Nucleon," Phys. Rev. Lett. **90**, 012001.
Guo, Yuxun, Xiangdong Ji, and Yizhuang Liu, 2021, "QCD analysis of near-threshold photon-proton production of heavy quarkonium," Phys. Rev. D **103**, 096010.
Guzey, V., and M. Siddikov, 2006, "On the A-dependence of nuclear generalized parton distributions," J. Phys. G **32**, 251–268.
Hägler, Ph, *et al.* (LHPC Collaboration), 2008, "Nucleon generalized parton distributions from full lattice QCD," Phys. Rev. D **77**, 094502.
Hatta, Yoshitaka, 2012, "Notes on the orbital angular momentum of quarks in the nucleon," Phys. Lett. B **708**, 186–190.
Hatta, Yoshitaka, Abha Rajan, and Kazuhiro Tanaka, 2018, "Quark and gluon contributions to the QCD trace anomaly," J. High Energy Phys. 12, 008.
Hatta, Yoshitaka, and Mark Strikman, 2021, "ϕ-meson lepto-production near threshold and the strangeness D-term," Phys. Lett. B **817**, 136295.
Hatta, Yoshitaka, and Di-Lun Yang, 2018, "Holographic J/ψ production near threshold and the proton mass problem," Phys. Rev. D **98**, 074003.
Heisenberg, W., 1932, "On the structure of atomic nuclei," Z. Phys. **77**, 1–11.
Higgs, Peter W., 2014, "Nobel Lecture: Evading the Goldstone theorem," Rev. Mod. Phys. **86**, 851.
Hoferichter, Martin, Jacobo Ruiz de Elvira, Bastian Kubis, and Ulf-G. Meißner, 2016, "Roy-Steiner-equation analysis of pion-nucleon scattering," Phys. Rep. **625**, 1–88.
't Hooft, Gerard, and M. J. G. Veltman, 1972, "Regularization and renormalization of gauge fields," Nucl. Phys. **B44**, 189–213.
Horn, Tanja, and Craig D. Roberts, 2016, "The pion: An enigma within the standard model," J. Phys. G **43**, 073001.
Hudson, Jonathan, and Peter Schweitzer, 2017, "D term and the structure of pointlike and composed spin-0 particles," Phys. Rev. D **96**, 114013.
Hwang, D. S., and Dieter Müller, 2008, "Implication of the overlap representation for modelling generalized parton distributions," Phys. Lett. B **660**, 350–359.
Ivanov, D. Yu., B. Pire, L. Szymanowski, and O. V. Teryaev, 2002, "Probing chiral-odd GPDs in diffractive electroproduction of two vector mesons," Phys. Lett. B **550**, 65–76.
Ivanov, D. Yu., A. Schäfer, L. Szymanowski, and G. Krasnikov, 2004, "Exclusive photoproduction of a heavy vector meson in QCD," Eur. Phys. J. C **34**, 297–316; **75**, 75(E) (2015).
Jaffe, R. L., and Aneesh Manohar, 1990, "The $G(1)$ Problem: Fact and fantasy on the spin of the proton," Nucl. Phys. **B337**, 509–546.
Ji, Xiangdong, 2013, "Parton Physics on a Euclidean Lattice," Phys. Rev. Lett. **110**, 262002.
Ji, Xiangdong, 2021, "Proton mass decomposition: Naturalness and interpretations," Front. Phys. **16**, 64601.
Ji, Xiangdong, and Yizhuang Liu, 2021, "Momentum-current gravitational multipoles of hadrons," arXiv:2110.14781.
Ji, Xiangdong, and Yizhuang Liu, 2022, "Gravitational tensor-monopole moment of hydrogen atom to order $\mathcal{O}(\alpha)$," arXiv:2208.05029.
Ji, Xiangdong, Feng Yuan, and Yong Zhao, 2021, "What we know and what we don't know about the proton spin after 30 years," Nat. Rev. Phys. **3**, 27–38.

Ji, Xiang-Dong, 1995a, "QCD Analysis of the Mass Structure of the Nucleon," Phys. Rev. Lett. **74**, 1071–1074.
Ji, Xiang-Dong, 1995b, "Breakup of hadron masses and energy-momentum tensor of QCD," Phys. Rev. D **52**, 271–281.
Ji, Xiang-Dong, 1997a, "Deeply virtual Compton scattering," Phys. Rev. D **55**, 7114–7125.
Ji, Xiang-Dong, 1997b, "Gauge-Invariant Decomposition of Nucleon Spin," Phys. Rev. Lett. **78**, 610–613.
Ji, Xiang-Dong, 1998, "Lorentz symmetry and the internal structure of the nucleon," Phys. Rev. D **58**, 056003.
Ji, Xiang-Dong, W. Melnitchouk, and X. Song, 1997, "Study of off-forward parton distributions," Phys. Rev. D **56**, 5511–5523.
Jo, H. S., *et al.* (CLAS Collaboration), 2015, "Cross Sections for the Exclusive Photon Electroproduction on the Proton and Generalized Parton Distributions," Phys. Rev. Lett. **115**, 212003.
Jung, Ju-Hyun, Ulugbek Yakhshiev, and Hyun-Chul Kim, 2014, "Energy-momentum tensor form factors of the nucleon within a soliton model," J. Phys. G **41**, 055107.
Jung, Ju-Hyun, Ulugbek Yakhshiev, Hyun-Chul Kim, and Peter Schweitzer, 2014, "In-medium modified energy-momentum tensor form factors of the nucleon within the framework of a π-ρ-ω soliton model," Phys. Rev. D **89**, 114021.
Kharzeev, D., 1996, "Quarkonium interactions in QCD," Proc. Int. Sch. Phys. "Enrico Fermi" **130**, 105–131.
Kharzeev, Dmitri E., 2021, "Mass radius of the proton," Phys. Rev. D **104**, 054015.
Kim, Hyun-Chul, Peter Schweitzer, and Ulugbek Yakhshiev, 2012, "Energy-momentum tensor form factors of the nucleon in nuclear matter," Phys. Lett. B **718**, 625–631.
Kim, June-Young, and Hyun-Chul Kim, 2021, "Energy-momentum tensor of the nucleon on the light front: Abel tomography case," Phys. Rev. D **104**, 074019.
Kim, June-Young, Hyun-Chul Kim, Maxim V. Polyakov, and Hyeon-Dong Son, 2021, "Strong force fields and stabilities of the nucleon and singly heavy baryon Σ_c," Phys. Rev. D **103**, 014015.
Kim, June-Young, and Bao-Dong Sun, 2021, "Gravitational form factors of a baryon with spin-3/2," Eur. Phys. J. C **81**, 85.
Kim, June-Young, Bao-Dong Sun, Dongyan Fu, and Hyun-Chul Kim, 2023, "Mechanical structure of a spin-1 particle," Phys. Rev. D **107**, 054007.
Kim, June-Young, Ulugbek Yakhshiev, and Hyun-Chul Kim, 2022, "Medium modification of the nucleon mechanical properties: Abel tomography case," Eur. Phys. J. C **82**, 719.
Kivel, N., Maxim V. Polyakov, and M. Vanderhaeghen, 2001, "Deeply virtual Compton scattering on the nucleon: Study of the twist-3 effects," Phys. Rev. D **63**, 114014.
Kobzarev, I. Yu., and L. B. Okun, 1962, "Gravitational interaction of fermions," Zh. Eksp. Teor. Fiz. **43**, 1904–1909, http://jetp.ras.ru/cgi-bin/dn/e_016_05_1343.pdf.
Kopeliovich, B. Z., Ivan Schmidt, and M. Siddikov, 2010, "Double deeply virtual Compton scattering on nucleons and nuclei," Phys. Rev. D **82**, 014017.
Kou, Wei, Rong Wang, and Xurong Chen, 2021, "Determination of the gluonic D-term and mechanical radii of proton from experimental data," arXiv:2104.12962.
Krutov, A. F., and V. E. Troitsky, 2021, "Pion gravitational form factors in a relativistic theory of composite particles," Phys. Rev. D **103**, 014029.
Krutov, A. F., and V. E. Troitsky, 2022, "Relativistic composite-particle theory of the gravitational form factors of the pion: Quantitative results," Phys. Rev. D **106**, 054013.
Kubis, Bastian, and Ulf-G. Meissner, 2000, "Virtual photons in the pion form-factors and the energy momentum tensor," Nucl. Phys. **A671**, 332–356; **A692**, 647(E)–648(E) (2001).
Kumano, S., Qin-Tao Song, and O. V. Teryaev, 2018, "Hadron tomography by generalized distribution amplitudes in pion-pair production process $\gamma^*\gamma \to \pi^0\pi^0$ and gravitational form factors for pion," Phys. Rev. D **97**, 014020.
Kumar, Narinder, Chandan Mondal, and Neetika Sharma, 2017, "Gravitational form factors and angular momentum densities in light-front quark-diquark model," Eur. Phys. J. A **53**, 237.
Kumerički, Krešimir, 2019, "Measurability of pressure inside the proton," Nature (London) **570**, E1–E2.
Kumerički, Krešimir, Simonetta Liuti, and Herve Moutarde, 2016, "GPD phenomenology and DVCS fitting: Entering the high-precision era," Eur. Phys. J. A **52**, 157.
Laue, M., 1911, "Zur Dynamik der Relativitätstheorie [On the dynamics of the theory of relativity]," Ann. Phys. (Berlin) **340**, 524–542.
Leader, E., and C. Lorcé, 2014, "The angular momentum controversy: What's it all about and does it matter?" Phys. Rep. **541**, 163–248.
Leutwyler, H., and Mikhail A. Shifman, 1989, "Goldstone bosons generate peculiar conformal anomalies," Phys. Lett. B **221**, 384–388.
Lin, Huey-Wen, 2021, "Nucleon Tomography and Generalized Parton Distribution at Physical Pion Mass from Lattice QCD," Phys. Rev. Lett. **127**, 182001.
Liu, Keh-Fei, 2021, "Proton mass decomposition and hadron cosmological constant," Phys. Rev. D **104**, 076010.
Liuti, S., and S. K. Taneja, 2005, "Nuclear medium modifications of hadrons from generalized parton distributions," Phys. Rev. C **72**, 034902.
Lorcé, Cédric, 2013a, "Geometrical approach to the proton spin decomposition," Phys. Rev. D **87**, 034031.
Lorcé, Cédric, 2013b, "Wilson lines and orbital angular momentum," Phys. Lett. B **719**, 185–190.
Lorcé, Cédric, 2018a, "On the hadron mass decomposition," Eur. Phys. J. C **78**, 120.
Lorcé, Cédric, 2018b, "The relativistic center of mass in field theory with spin," Eur. Phys. J. C **78**, 785.
Lorcé, Cédric, 2020, "Charge Distributions of Moving Nucleons," Phys. Rev. Lett. **125**, 232002.
Lorcé, Cédric, 2021, "Relativistic spin sum rules and the role of the pivot," Eur. Phys. J. C **81**, 413.
Lorcé, Cédric, and Peter Lowdon, 2020, "Universality of the Poincaré gravitational form factor constraints," Eur. Phys. J. C **80**, 207.
Lorcé, Cédric, Luca Mantovani, and Barbara Pasquini, 2018, "Spatial distribution of angular momentum inside the nucleon," Phys. Lett. B **776**, 38–47.
Lorcé, Cédric, Andreas Metz, Barbara Pasquini, and Simone Rodini, 2021, "Energy-momentum tensor in QCD: Nucleon mass decomposition and mechanical equilibrium," J. High Energy Phys. 11, 121.
Lorcé, Cédric, Hervé Moutarde, and Arkadiusz P. Trawiński, 2019, "Revisiting the mechanical properties of the nucleon," Eur. Phys. J. C **79**, 89.
Lorcé, Cédric, Bernard Pire, and Qin-Tao Song, 2022, "Kinematical higher-twist corrections in $\gamma^*\gamma \to M\bar{M}$," Phys. Rev. D **106**, 094030.
Lorcé, Cédric, Peter Schweitzer, and Kemal Tezgin, 2022, "2D energy-momentum tensor distributions of nucleon in a large-N_c quark model from ultrarelativistic to nonrelativistic limit," Phys. Rev. D **106**, 014012.

Lowdon, Peter, Kelly Yu-Ju Chiu, and Stanley J. Brodsky, 2017, "Rigorous constraints on the matrix elements of the energy-momentum tensor," Phys. Lett. B **774**, 1–6.

Ma, Yan-Qing, and Jian-Wei Qiu, 2018, "Exploring Partonic Structure of Hadrons Using *Ab Initio* Lattice QCD Calculations," Phys. Rev. Lett. **120**, 022003.

Mai, Manuel, and Peter Schweitzer, 2012a, "Energy momentum tensor, stability, and the D-term of Q-balls," Phys. Rev. D **86**, 076001.

Mai, Manuel, and Peter Schweitzer, 2012b, "Radial excitations of Q-balls, and their D-term," Phys. Rev. D **86**, 096002.

Mamo, Kiminad A., and Ismail Zahed, 2020, "Diffractive photoproduction of J/ψ and Υ using holographic QCD: Gravitational form factors and GPD of gluons in the proton," Phys. Rev. D **101**, 086003.

Mamo, Kiminad A., and Ismail Zahed, 2021, "Nucleon mass radii and distribution: Holographic QCD, lattice QCD, and GlueX data," Phys. Rev. D **103**, 094010.

Mamo, Kiminad A., and Ismail Zahed, 2022, "J/ψ near threshold in holographic QCD: A and D gravitational form factors," Phys. Rev. D **106**, 086004.

Masuda, M., *et al.* (Belle Collaboration), 2016, "Study of π^0 pair production in single-tag two-photon collisions," Phys. Rev. D **93**, 032003.

McAllister, R. W., and R. Hofstadter, 1956, "Elastic scattering of 188-MeV electrons from the proton and the α particle," Phys. Rev. **102**, 851–856.

Mecking, B. A., *et al.* (CLAS Collaboration), 2003, "The CEBAF Large Acceptance Spectrometer (CLAS)," Nucl. Instrum. Methods Phys. Res., Sect. A **503**, 513–553.

Metz, Andreas, Barbara Pasquini, and Simone Rodini, 2020, "Revisiting the proton mass decomposition," Phys. Rev. D **102**, 114042.

Metz, Andreas, Barbara Pasquini, and Simone Rodini, 2021, "The gravitational form factor $D(t)$ of the electron," Phys. Lett. B **820**, 136501.

Mondal, Chandan, 2016, "Longitudinal momentum densities in transverse plane for nucleons," Eur. Phys. J. C **76**, 74.

Mondal, Chandan, Narinder Kumar, Harleen Dahiya, and Dipankar Chakrabarti, 2016, "Charge and longitudinal momentum distributions in transverse coordinate space," Phys. Rev. D **94**, 074028.

More, Jai, Asmita Mukherjee, Sreeraj Nair, and Sudeep Saha, 2022, "Gravitational form factors and mechanical properties of a quark at one loop in light-front Hamiltonian QCD," Phys. Rev. D **105**, 056017.

More, Jai, Asmita Mukherjee, Sreeraj Nair, and Sudeep Saha, 2023, "Gluon contribution to the mechanical properties of a dressed quark in light-front Hamiltonian QCD," arXiv:2302.11906.

Müller, Dieter, Tobias Lautenschlager, Kornelija Passek-Kumerički, and Andreas Schäfer, 2014, "Towards a fitting procedure to deeply virtual meson production—The next-to-leading order case," Nucl. Phys. **B884**, 438–546.

Müller, Dieter, D. Robaschik, B. Geyer, F. M. Dittes, and J. Hořejši, 1994, "Wave functions, evolution equations and evolution kernels from light ray operators of QCD," Fortschr. Phys. **42**, 101–141.

Nambu, Yoichiro, and G. Jona-Lasinio, 1961a, "Dynamical model of elementary particles based on an analogy with superconductivity. I," Phys. Rev. **122**, 345–358.

Nambu, Yoichiro, and G. Jona-Lasinio, 1961b, "Dynamical model of elementary particles based on an analogy with superconductivity. II," Phys. Rev. **124**, 246–254.

Neubelt, Matt J., Andrew Sampino, Jonathan Hudson, Kemal Tezgin, and Peter Schweitzer, 2020, "Energy momentum tensor and the D-term in the bag model," Phys. Rev. D **101**, 034013.

Nielsen, N. K., 1977, "The energy-momentum tensor in a non-Abelian quark gluon theory," Nucl. Phys. **B120**, 212–220.

Noether, Emmy, 1918, "Invariant variation problems," Gott. Nachr. 235–257 [arXiv:physics/0503066v3].

Novikov, V. A., and Mikhail A. Shifman, 1981, "Comment on the $\psi' \to J/\psi\pi\pi$ decay," Z. Phys. C **8**, 43.

Ossmann, J., M. V. Polyakov, P. Schweitzer, D. Urbano, and K. Goeke, 2005, "Generalized parton distribution function $(E^u + E^d)(x, \xi, t)$ of the nucleon in the chiral quark soliton model," Phys. Rev. D **71**, 034011.

Owa, Shiryo, A. W. Thomas, and X. G. Wang, 2022, "Effect of the pion field on the distributions of pressure and shear in the proton," Phys. Lett. B **829**, 137136.

Özdem, U., and K. Azizi, 2020, "Gravitational form factors of hyperons in light-cone QCD," Phys. Rev. D **101**, 114026.

Özel, Feryal, and Paulo Freire, 2016, "Masses, radii, and the equation of state of neutron stars," Annu. Rev. Astron. Astrophys. **54**, 401–440.

Pagels, Heinz, 1966, "Energy-momentum structure form factors of particles," Phys. Rev. **144**, 1250–1260.

Panteleeva, Julia Yu., and Maxim V. Polyakov, 2020, "Quadrupole pressure and shear forces inside baryons in the large N_c limit," Phys. Lett. B **809**, 135707.

Panteleeva, Julia Yu., and Maxim V. Polyakov, 2021, "Forces inside the nucleon on the light front from 3D Breit frame force distributions: Abel tomography case," Phys. Rev. D **104**, 014008.

Pasquini, B., and S. Boffi, 2007, "Nucleon spin densities in a light-front constituent quark model," Phys. Lett. B **653**, 23–28.

Pasquini, B., M. V. Polyakov, and M. Vanderhaeghen, 2014, "Dispersive evaluation of the D-term form factor in deeply virtual Compton scattering," Phys. Lett. B **739**, 133–138.

Pedrak, A., B. Pire, L. Szymanowski, and J. Wagner, 2020, "Electroproduction of a large invariant mass photon pair," Phys. Rev. D **101**, 114027.

Pefkou, Dimitra A., Daniel C. Hackett, and Phiala E. Shanahan, 2022, "Gluon gravitational structure of hadrons of different spin," Phys. Rev. D **105**, 054509.

Perevalova, I. A., M. V. Polyakov, and P. Schweitzer, 2016, "On LHCb pentaquarks as a baryon-$\psi(2S)$ bound state: prediction of isospin-3/2 pentaquarks with hidden charm," Phys. Rev. D **94**, 054024.

Petrov, V. Yu., P. V. Pobylitsa, Maxim V. Polyakov, I. Börnig, K. Goeke, and C. Weiss, 1998, "Off-forward quark distributions of the nucleon in the large-N_c limit," Phys. Rev. D **57**, 4325–4333.

Pire, B., L. Szymanowski, and J. Wagner, 2011, "NLO corrections to timelike, spacelike and double deeply virtual Compton scattering," Phys. Rev. D **83**, 034009.

Politzer, H. David, 1973, "Reliable Perturbative Results for Strong Interactions?," Phys. Rev. Lett. **30**, 1346–1349.

Polyakov, Maxim V., 2003, "Generalized parton distributions and strong forces inside nucleons and nuclei," Phys. Lett. B **555**, 57–62.

Polyakov, Maxim V., and Peter Schweitzer, 2018a, "D-term, strong forces in the nucleon, and their applications," arXiv:1801.05858.

Polyakov, Maxim V., and Peter Schweitzer, 2018b, "Forces inside hadrons: Pressure, surface tension, mechanical radius, and all that," Int. J. Mod. Phys. A **33**, 1830025.

Polyakov, Maxim V., and Hyeon-Dong Son, 2018, "Nucleon gravitational form factors from instantons: Forces between quark and gluon subsystems," J. High Energy Phys. 09, 156.

Polyakov, Maxim V., and Bao-Dong Sun, 2019, "Gravitational form factors of a spin one particle," Phys. Rev. D **100**, 036003.
Polyakov, Maxim V., and C. Weiss, 1999, "Skewed and double distributions in pion and nucleon," Phys. Rev. D **60**, 114017.
Prakash, Madappa, James M. Lattimer, Jose A. Pons, Andrew W. Steiner, and Sanjay Reddy, 2001, "Evolution of a neutron star from its birth to old age," Lect. Notes Phys. **578**, 364–423.
Qiu, Jian-Wei, and Zhite Yu, 2022, "Exclusive production of a pair of high transverse momentum photons in pion-nucleon collisions for extracting generalized parton distributions," J. High Energy Phys. 08, 103.
Radyushkin, A. V., 1996, "Scaling limit of deeply virtual Compton scattering," Phys. Lett. B **380**, 417–425.
Radyushkin, A. V., 2017, "Quasi-parton distribution functions, momentum distributions, and pseudo-parton distribution functions," Phys. Rev. D **96**, 034025.
Raya, Khepani, Zhu-Fang Cui, Lei Chang, Jose-Manuel Morgado, Craig D. Roberts, and Jose Rodriguez-Quintero, 2022, "Revealing pion and kaon structure via generalised parton distributions," Chin. Phys. C **46**, 013105.
Rodini, S., A. Metz, and B. Pasquini, 2020, "Mass sum rules of the electron in quantum electrodynamics," J. High Energy Phys. 09, 067.
Rutherford, E., 1919, "Collision of α particles with light atoms. IV. An anomalous effect in nitrogen," Philos. Mag. Ser. 6 **37**, 581–587.
Sachs, R. G., 1962, "High-energy behavior of nucleon electromagnetic form factors," Phys. Rev. **126**, 2256–2260.
Schweitzer, P., S. Boffi, and M. Radici, 2002, "Polynomiality of unpolarized off forward distribution functions and the D term in the chiral quark soliton model," Phys. Rev. D **66**, 114004.
Shanahan, P. E., and W. Detmold, 2019a, "Gluon gravitational form factors of the nucleon and the pion from lattice QCD," Phys. Rev. D **99**, 014511.
Shanahan, P. E., and W. Detmold, 2019b, "Pressure Distribution and Shear Forces inside the Proton," Phys. Rev. Lett. **122**, 072003.
Shifman, Mikhail A., A. I. Vainshtein, and Valentin I. Zakharov, 1978, "Remarks on Higgs boson interactions with nucleons," Phys. Lett. B **78**, 443–446.
Snow, G. A., and M. M. Shapiro, 1961, "Mesons and hyperons," Rev. Mod. Phys. **33**, 231.
Son, Hyeon-Dong, and Hyun-Chul Kim, 2014, "Stability of the pion and the pattern of chiral symmetry breaking," Phys. Rev. D **90**, 111901.
Stepanyan, S., *et al.* (CLAS Collaboration), 2001, "Observation of Exclusive Deeply Virtual Compton Scattering in Polarized Electron Beam Asymmetry Measurements," Phys. Rev. Lett. **87**, 182002.
Sun, Bao-Dong, and Yu-Bing Dong, 2020, "Gravitational form factors of ρ meson with a light-cone constituent quark model," Phys. Rev. D **101**, 096008.
Sun, Peng, Xuan-Bo Tong, and Feng Yuan, 2021, "Perturbative QCD analysis of near threshold heavy quarkonium photoproduction at large momentum transfer," Phys. Lett. B **822**, 136655.
Sun, Peng, Xuan-Bo Tong, and Feng Yuan, 2022, "Near threshold heavy quarkonium photoproduction at large momentum transfer," Phys. Rev. D **105**, 054032.
Suzuki, Hiroshi, 2013, "Energy-momentum tensor from the Yang-Mills gradient flow," Prog. Theor. Exp. Phys. 083B03; (2015) 079201(E).
Tanaka, Kazuhiro, 2018, "Operator relations for gravitational form factors of a spin-0 hadron," Phys. Rev. D **98**, 034009.
Tanaka, Kazuhiro, 2019, "Three-loop formula for quark and gluon contributions to the QCD trace anomaly," J. High Energy Phys. 01, 120.
Tanaka, Kazuhiro, 2023, "Twist-four gravitational form factor at NNLO QCD from trace anomaly constraints," J. High Energy Phys. 03, 013.
Teryaev, O. V., 1999, "Spin structure of nucleon and equivalence principle," arXiv:hep-ph/9904376.
Teryaev, O. V., 2001, "Crossing and radon tomography for generalized parton distributions," Phys. Lett. B **510**, 125–132.
Tong, Xuan-Bo, Jian-Ping Ma, and Feng Yuan, 2021, "Gluon gravitational form factors at large momentum transfer," Phys. Lett. B **823**, 136751.
Tong, Xuan-Bo, Jian-Ping Ma, and Feng Yuan, 2022, "Perturbative calculations of gravitational form factors at large momentum transfer," J. High Energy Phys. 10, 046.
Vanderhaeghen, M., Pierre A. M. Guichon, and M. Guidal, 1999, "Deeply virtual electroproduction of photons and mesons on the nucleon: Leading order amplitudes and power corrections," Phys. Rev. D **60**, 094017.
Varma, Mira, and Peter Schweitzer, 2020, "Effects of long-range forces on the D-term and the energy-momentum structure," Phys. Rev. D **102**, 014047.
Voloshin, M. B., and A. D. Dolgov, 1982, "On gravitational interaction of the Goldstone bosons," Sov. J. Nucl. Phys. **35**, 120–121.
Voloshin, Mikhail B., and Valentin I. Zakharov, 1980, "Measuring QCD Anomalies in Hadronic Transitions between Onium States," Phys. Rev. Lett. **45**, 688.
Wakamatsu, M., 2007, "On the D-term of the nucleon generalized parton distributions," Phys. Lett. B **648**, 181–185.
Wakamatsu, Masashi, 2014, "Is gauge-invariant complete decomposition of the nucleon spin possible?," Int. J. Mod. Phys. A **29**, 1430012.
Wang, Gen, Yi-Bo Yang, Jian Liang, Terrence Draper, and Keh-Fei Liu (χQCD Collaboration) 2022, "Proton momentum and angular momentum decompositions with overlap fermions," Phys. Rev. D **106**, 014512.
Wang, Xiao-Yun, Fancong Zeng, and Quanjin Wang, 2022, "Gluon gravitational form factors and mechanical properties of proton," arXiv:2208.03186.
Witten, Edward, 1979, "Baryons in the $1/N$ expansion," Nucl. Phys. **B160**, 57–115.
Won, Ho-Yeon, June-Young Kim, and Hyun-Chul Kim, 2022, "Gravitational form factors of the baryon octet with flavor SU(3) symmetry breaking," Phys. Rev. D **106**, 114009.
Workman, R. L., *et al.* (Particle Data Group), 2022, "Review of particle physics," Prog. Theor. Exp. Phys. 083C01.
Yang, Yi-Bo, Ming Gong, Jian Liang, Huey-Wen Lin, Keh-Fei Liu, Dimitra Pefkou, and Phiala Shanahan, 2018, "Nonperturbatively renormalized glue momentum fraction at the physical pion mass from lattice QCD," Phys. Rev. D **98**, 074506.
Yang, Yi-Bo, Jian Liang, Yu-Jiang Bi, Ying Chen, Terrence Draper, Keh-Fei Liu, and Zhaofeng Liu, 2018, "Proton Mass Decomposition from the QCD Energy Momentum Tensor," Phys. Rev. Lett. **121**, 212001.
Yang, Yi-Bo, Raza Sabbir Sufian, Andrei Alexandru, Terrence Draper, Michael J. Glatzmaier, Keh-Fei Liu, and Yong Zhao, 2017, "Glue Spin and Helicity in the Proton from Lattice QCD," Phys. Rev. Lett. **118**, 102001.
Zweig, G., 1964, "An SU(3) model for strong interaction symmetry and its breaking. Version 1," CERN Report No. CERN-TH-401.